PHYSICAL REVIEW D **90,** 096006 (2014)

Testing new physics effects in $B \to K^* \ell^+ \ell^-$

Rusa Mandal[*] and Rahul Sinha[†]
The Institute of Mathematical Sciences, Taramani, Chennai 600113, India

Diganta Das[‡]
Institut für Physik, Technische Universität Dortmund, D-44221 Dortmund, Germany
(Received 18 September 2014; published 12 November 2014)

It is generally believed that the decay mode $B \to K^* \ell^+ \ell^-$ is one of the best modes to search for physics beyond the standard model. The angular distribution enables the independent measurement of several observables as a function of the dilepton invariant mass. The plethora of observables so obtained enable unique tests of the standard model contributions. We start by writing the most general parametric form of the standard model amplitude for $B \to K^* \ell^+ \ell^-$ taking into account comprehensively all contributions within the standard model. These include all short-distance and long-distance effects, factorizable and nonfactorizable contributions, complete electromagnetic corrections to hadronic operators up to all orders, resonance contributions and the finite lepton and quark masses. The parametric form of the amplitude in the standard model results a new relation involving all the *CP* conserving observables. The derivation of this relation only needs the parametric form of the amplitude and not a detailed calculation of it. Hence, we make no approximations, however, innocuous. The violation of this relation will provide a smoking gun signal of new physics. We use the 1 fb^{-1} LHC*b* data to explicitly show how our relation can be used to test standard model and search for new physics that might contribute to this decay.

DOI: 10.1103/PhysRevD.90.096006 PACS numbers: 11.30.Er, 13.25.Hw, 12.60.-i

I. INTRODUCTION

It is a historical fact that several discoveries in particle physics were preceded by indirect evidence through quantum loop contributions. It is for this reason that significant attention is devoted to studying loop processes. The muon magnetic moment is one of the best examples of such a process where precision calculations have been done in order to search for new physics by comparing the theoretical expectation with experimental observation. It is a testimony to such searches for new physics (NP) beyond the standard model (SM) that both theoretical estimates and experimental observation have reached a precision where the hadronic effects even for the lepton magnetic moment dominate the discrepancy between theory and observation. Indirect searches for new physics often involve precision measurement of a single quantity that is compared to a theoretical estimate that also needs to be very accurately calculated. Unfortunately, hadronic estimates involve calculation of long-distance QCD effects which cannot easily be done accurately, limiting the scope of such searches. There exist, however, certain decay modes which involve the measurement of several observables that can be related to each other with minimal assumptions and completely calculable QCD contributions within the SM. The breakdown of such relation(s) between observables would unambiguously signal the presence of NP. Such tests are by nature not limited by incalculable hadronic effects and hence provide an unambiguous signal of NP. A well-known example [1,2] of such a process is the semileptonic penguin decay $B \to K^* \ell^+ \ell^-$, where ℓ is either the electron or the muon. In this paper we will show how this decay, which occurs in multiple partial waves, can be used to obtain reliable tests of NP.

Flavor changing neutral current transitions are well known to be sensitive to NP contributions. However, hadronic flavor changing neutral current receive short- and long-distance QCD contributions that are not easy to estimate reliably. It is evident from the data collected by the Belle, *BABAR* and CMS Collaborations at the B-factories, CLEO, CDF, Tevatron and LHC*b* that NP does not show up as a large and unambiguous effect. This has bought into focus the need for approaches that are theoretically cleaner i.e., where the hadronic uncertainties are much smaller than the effects of NP that are being probed. Hence, to effectively search for NP it is crucial to separate the effect of new physics from hadronic uncertainties that can contribute to the decay. The decay mode $B \to K^* \ell^+ \ell^-$ is regarded [2] as significant in this attempt. The full angular analysis of the final state gives rise to a multitude of observables [1,3] that are related as they arise from the same decay mode. In addition, each of these observables can be measured as function of the dilepton invariant mass. In Ref. [2] an interesting relation between the various observables that can be measured in this mode was derived. The derivation was based on a few assumptions that are

[*]rusam@imsc.res.in
[†]sinha@imsc.res.in
[‡]diganta.das@tu-dortmund.de

reasonable. These included ignoring the mass of the lepton ℓ and the s-quark that appears in the short-distance Hamiltonian describing the decay. The decay amplitude was assumed to be real, thereby ignoring the extremely tiny CP violation, the small imaginary contribution to the amplitude that arises from the Wilson coefficient C_9 which is complex in general and the dilepton resonances which were presumed to be removed from the experimental analysis. These assumptions reduced the number of nonzero observables to only six. In this paper, we carefully *redo the analysis without making any kind of approximation, however, innocuous*. Our approach once again is to derive the most general parametric form of the decay amplitude, which results in a relation between the several related observables.

In this paper we generalize the derivation in Ref. [2] to incorporate a complex decay amplitude, eliminating the need to ignore imaginary contributions arising from C_9 and ensuring that the new relation is valid even when resonance contributions are not excluded from the (experimental) analysis. This implies that the new relation derived in this paper involves all the nine CP conserving observables that can be measured using this mode. The derivation of the new relation does not depend on theoretical values of the Wilson coefficients and does not require making any assumptions on the form factors; in particular we do not limit the form factor to any power of $\Lambda_{\rm QCD}/m_b$ expansion in heavy quark effect theory (HQET) [4]. In fact, the derivation of the new relation itself does not require HQET. The new derivation parametrically incorporates all short-distance and long-distance effects including resonance contributions, as well as, factorizable and nonfactorizable contributions. We also include complete electromagnetic (EM) corrections to hadronic operators up to all orders. Finally, we retain the lepton mass and the s-quark mass. We envisage that the derivation to be exact in all respects and the new relation obtained here to be one of the cleanest tests of the SM in B decays.

The LHCb Collaboration has measured [5] all the possible CP conserving observables through an angular analysis. These independent measurements consist of the differential decay rate with respect to the dilepton invariant mass, two independent helicity fractions and six angular asymmetries. Three of the asymmetries are zero unless there exist imaginary contributions to the decay amplitudes. If these asymmetries are measured to be zero in the future, the relation between the observables would be free from any hadronic parameter as derived in Ref. [2]. While these asymmetries are currently measured to be small and consistent with zero, there could, however, exist contributions from wide resonances which might still be permitted within statistical errors. Including these asymmetries in the analysis to account for complex amplitudes results in a modification of the relation purely between observables. The modifying terms now involve a single hadronic parameter in addition to being proportional to the three asymmetries. Hence, SM can be tested or equivalently NP contributions can be probed reliably with the knowledge of just one hadronic parameter. It is interesting that all effort to estimate long- and short-distance QCD contributions now need to be focused only on accurately estimating this single parameter. Since the asymmetries involved in modifying terms (which arise from complex amplitudes) are already constrained to be small, the results are not very sensitive to the single hadronic parameter. We find that the inclusion of imaginary contributions to the amplitude must always reduce the parameter space. This would enhance any discrepancy that may be observed even when the imaginary part of the amplitudes are ignored. We use the 1 fb^{-1} LHCb data to show how our relation can be used to test standard model and find new physics that might contribute to this decay.

In this paper we review the theoretical framework required to describe $B \to K^* \ell^+ \ell^-$ and derive the most general parametric form of the amplitude describing the decay in Sec. II. The amplitude written is notionally exact in all respects. In Sec. III we construct all the observables in terms of the amplitude derived in Sec. II. Here we retain the lepton mass as well as the strange quark mass that appears in the short-distance Hamiltonian describing this decay. A new relation between observables is derived in Sec. IV under the assumption of massless lepton, but retaining all other effects and contribution. In Sec. V we generalize the new relation derived in Sec. IV to include the mass of the lepton that had been ignored earlier. We rederive two simple limits of the relation between observables that hold at zero crossings of other asymmetries such as the forward-backward asymmetry. The values of all the observables at kinematic endpoints of the dilepton invariant mass are easily understood in Sec. VI. A numerical analysis is presented in Sec. VII that tests the validity of the relation derived assuming SM. We discuss the constraints already imposed by the 1 fb^{-1} LHCb data [5], but refrain from drawing even the obvious conclusions given that results for 3 fb^{-1} data will soon be presented. In Sec. VIII we summarize the significant results obtained in our paper.

II. THEORETICAL FRAMEWORK

In this section we will discuss the most general from of the amplitude that can describe the exclusive decay mode $B \to K^* \ell^+ \ell^-$ in the SM. The description of the decay $B \to K^* \ell^+ \ell^-$ requires as the first step the separation of short-distance effects which involve perturbative QCD and weak interaction from the long-distance QCD contributions in an effective Hamiltonian. As is well explained in literature, exclusive decay modes are a challenge to describe theoretically. This difficulty arises not only in the need to know hadronic form factors accurately but also from the existence of "nonfactorizable" contributions that do not correspond to form factors. These contributions

originate from electromagnetic corrections to the matrix element of purely hadronic operators in the effective Hamiltonian. It has been demonstrated [6] that these nonfactorizable corrections can be computed allowing exclusive decay such as $B \to K^*\gamma$ and $B \to K^*\ell^+\ell^-$ to be treated systematically much as their inclusive decay counterparts. It is based on this theoretical understanding that we will write the most general from of the amplitude for $B \to K^*\ell^+\ell^-$ in the SM. Our approach will be to examine the various factorizable and nonfactorizable contributions to the process and write the most general parametric form of the amplitude without making any attempt to evaluate it.

The decays $B \to K^*\ell^+\ell^-$ occurs at the quark level via a $b \to s\ell^+\ell^-$ flavor changing neutral current transition. The short-distance effective Hamiltonian for the inclusive process $b \to s\ell^+\ell^-$ is given in the SM by [7–9]

$$\mathcal{H}_{\rm eff} = -4\frac{G_F}{\sqrt{2}}\Bigg[V_{tb}V_{ts}^*\Bigg(C_1\mathcal{O}_1^c + C_2\mathcal{O}_2^c + \sum_{i=3}^{10} C_i\mathcal{O}_i\Bigg) + V_{ub}V_{us}^*(C_1(\mathcal{O}_1^c - \mathcal{O}_1^u) + C_2(\mathcal{O}_2^c - \mathcal{O}_2^u))\Bigg]. \quad (1)$$

The local operators $\mathcal{O}_i$ are as given in Ref. [8], however, for completeness we present the relevant operators that are dominant:

$$\mathcal{O}_7 = \frac{e}{g^2}[\bar{s}\sigma_{\mu\nu}(m_bP_R + m_sP_L)b]F^{\mu\nu},$$
$$\mathcal{O}_9 = \frac{e^2}{g^2}(\bar{s}\gamma_\mu P_L b)\bar{\ell}\gamma^\mu\ell,$$
$$\mathcal{O}_{10} = \frac{e^2}{g^2}(\bar{s}\gamma_\mu P_L b)\bar{\ell}\gamma^\mu\gamma_5\ell,$$

where $g(e)$ is the strong (electromagnetic)coupling constant, $P_{L,R} = (1 \mp \gamma_5)/2$ are the left and right chiral projection operators and $m_b(m_s)$ are the running $b(s)$ quark mass in the $\overline{\rm MS}$ scheme. The Wilson coefficients C_i encode all the short-distance effects and are calculated in perturbation theory at a matching scale $\mu = M_W$ up to desired order in the strong coupling constant α_s before being evolved down to the scale $\mu = m_b \approx 4.8$ GeV. All NP contributions to $B \to K^*\ell^+\ell^-$ contribute exclusively to C_i; this includes new Wilson coefficients corresponding to new operators that arise from NP.

Significant effort (see Refs. [10,11] for reviews) has gone into evaluating the Wilson coefficients up to next-to-next-to-leading-logarithmic (NNLL) order. As has been stressed earlier [11] it is important to remember that "the construction of the effective Hamiltonian by means of operator product expansion and renormalization group methods can be done fully in the perturbative framework. The fact that the decaying hadron are bound states of quarks is irrelevant for this construction." This implies that the C_i are decay mode independent. The dependence on the mode enters only through the matrix element of local bilinear quark operators $\mathcal{O}_i$, i.e. $\langle f|\mathcal{O}_i|B\rangle$, which encodes the long-distance contributions. Since the decay amplitude cannot depend on the scale μ, $\langle f|\mathcal{O}_i|B\rangle$ must depend on the scale μ as well. The cancellation of μ dependence generally involves several terms in the operator product expansion. Since the calculation of the hadronic matrix element involves long-distance contributions, nonperturbative methods are required. Much progress has been made in these calculations using HQET as a tool. However, the dominant theoretical error in the amplitude arises due to the lack of reliable calculations of the hadron matrix element.

The simple picture of the decay presented above is unfortunately not accurate enough; there exist several corrections making a reliable estimate of the decay amplitude a challenge. The difficulty goes beyond accurately estimating the form factors involved in the hadron matrix element. There exist [6] additional nonfactorizable and long-distance contributions which arise from electromagnetic corrections to the matrix elements of purely hadronic operators in the Hamiltonian that cannot be absorbed into hadronic form factors. These contributions are generated by current-current operators $\mathcal{O}_{1,2}$ and penguin operators $\mathcal{O}_{3\text{–}6,8}$, combined with electromagnetic interaction of quarks to produce $\ell^+\ell^-$. The complication in dealing with these corrections is that the average distances between the photon emission and the weak interaction points are not necessarily short resulting in essentially nonlocal contributions to the decay amplitude which cannot be reduced to local form factors. A further challenge is that each such contribution has to identified and estimated one by one. The intermediate charm quark (and in principle the up quark) loops can couple to lepton pairs via a virtual photon and even though these effects are subdominant numerically in certain kinematical regions, they cannot be completely neglected. The other quarks contribute negligibly (except for resonant contribution which we will discuss later) to $\mathcal{O}_{1,2}$ and penguin operators $\mathcal{O}_{3\text{–}6,8}$ for $B \to K^*\ell^+\ell^-$ as they are either Cabibbo-Kobayashi-Maskawa (CKM) suppressed or have small accompanying Wilson coefficient. A remarkable effort [12,13] has gone into understanding the details of the hadronic contributions in B decays and in particular to $B \to K^*\ell^+\ell^-$. It is fortunate that the remarkable progress made so far enables us to write a completely accurate parametric form of the amplitude for this mode in the SM.

LHC*b* has observed a broad peaking structure [14,15] in the dimuon spectrum of $B \to K\ell^+\ell^-$. It would be of interest to see if this observation of broad resonances has implication on $B \to K^*\ell^+\ell^-$ mode, since long-distance effects would have to be included systematically. The decay mode $B \to K^*\ell^+\ell^-$ carries more information [1,3] on the dynamics as compared to the counterpart pseudoscalar mode $B \to K\ell^+\ell^-$, since the K^* polarization can also be measured. In order to study the dependence of the

amplitude on the helicity of the K^* we further consider the decay $K^* \to K\pi$ or the decay process $B \to K^*\ell^+\ell^- \to (K\pi)_{K^*}\ell^+\ell^-$. This further step itself does not complicate matters. The decay amplitude in terms of hadronic matrix elements must therefore include direct contributions proportional to C_7, C_9 and C_{10} multiplied by $B \to K^*$ form factors and contributions from nonlocal hadronic matrix elements $\mathcal{H}_i$ such that [16,17],

$$A(B(p) \to K^*(k)\ell^+\ell^-) = \frac{G_F\alpha}{\sqrt{2}\pi}V_{tb}V_{ts}^*\Bigg[\Bigg\{\hat{C}_9\langle K^*|\bar{s}\gamma^\mu P_L b|\bar{B}\rangle - \frac{2\hat{C}_7}{q^2}\langle K^*|\bar{s}i\sigma^{\mu\nu}q_\nu(m_b P_R + m_s P_L)b|\bar{B}\rangle - \frac{16\pi^2}{q^2}\sum_{i=\{1-6,8\}}\hat{C}_i\mathcal{H}_i^\mu\Bigg\}\bar{\ell}\gamma_\mu\ell + \hat{C}_{10}\langle K^*|\bar{s}\gamma^\mu P_L b|\bar{B}\rangle\bar{\ell}\gamma_\mu\gamma_5\ell\Bigg], \tag{2}$$

where, $p = q + k$ with q being the dilepton invariant momentum and the nonlocal hadron matrix element $\mathcal{H}_i^\mu$ is given by

$$\mathcal{H}_i^\mu = \langle K^*(k)|i\int d^4x e^{iq\cdot x}T\{j_{em}^\mu(x), \mathcal{O}_i(0)\}|\bar{B}(p)\rangle.$$

In Eq. (2), we have introduced *new notional theoretical parameters $\hat{C}_7$, $\hat{C}_9$ and $\hat{C}_{10}$ to indicate the true values of Wilson coefficients, which are by definition not dependent on the order of the perturbative calculation to which they are evaluated*. Our definition is explicit and should not be confused with those defined earlier in literature. The amplitude expressed in Eq. (2) is *notionally complete and free from any approximations*. In this paper we do not attempt to estimate the hadronic matrix element involved in Eq. (2), instead we use Lorentz invariance to write out the most general form of the hadron matrix elements $\langle K^*|\bar{s}\gamma^\mu P_L b|\bar{B}(p)\rangle$ and $\langle K^*|\bar{s}i\sigma^{\mu\nu}q_\nu P_{R,L}b|\bar{B}(p)\rangle$ which may be defined as

$$\langle K^*(\epsilon^*,k))|\bar{s}\gamma^\mu P_L b|B(p)\rangle = \epsilon_\nu^*\left(\mathcal{X}_0 q^\mu q^\nu + \mathcal{X}_1\left(g^{\mu\nu} - \frac{q^\mu q^\nu}{q^2}\right) + \mathcal{X}_2\left(k^\mu - \frac{k.q}{q^2}q^\mu\right)q^\nu + i\mathcal{X}_3\epsilon^{\mu\nu\rho\sigma}k_\rho q_\sigma\right), \tag{3}$$

$$\langle K^*(\epsilon^*,k))|i\bar{s}\sigma^{\mu\nu}q_\nu P_{R,L}b|B(p)\rangle = \epsilon_\nu^*\left(\pm\mathcal{Y}_1\left(g^{\mu\nu} - \frac{q^\mu q^\nu}{q^2}\right) \pm \mathcal{Y}_2\left(k^\mu - \frac{k.q}{q^2}q^\mu\right)q^\nu + i\mathcal{Y}_3\epsilon^{\mu\nu\rho\sigma}k_\rho q_\sigma\right). \tag{4}$$

We have written Eq. (3) such that the vector part of the current in $\langle K^*(\epsilon^*,k))|\bar{s}\gamma^\mu P_L b|B(p)\rangle$ is conserved and only the $\mathcal{X}_0$ term in the divergence of the axial part survives. Equation (4) is also written so as to ensure that $\langle K^*|i\bar{s}\sigma^{\mu\nu}q_\nu P_{R,L}b|B\rangle q_\mu = 0$. The relations between $\mathcal{X}_{0,1,2,3}$ and $\mathcal{Y}_{1,2,3}$ and the form factors conventionally defined for on-shell K^* are discussed in Appendix B. It should be noted that form factors $\mathcal{X}_{0,1,2,3}$ and $\mathcal{Y}_{1,2,3}$ are functions of q^2 and k^2, but we suppress the explicit dependence for simplicity of notation. The subsequent decay of the K^*, i.e., $K^*(k) \to K(k_1)\pi(k_2)$ can be easily taken into account [1,8] resulting in the hadronic matrix element $\langle[K(k_1)\pi(k_2)]_{K^*}|\bar{s}\gamma^\mu P_L b|B(p)\rangle$ being written as

$$\langle[K(k_1)\pi(k_2)]_{K^*}|\bar{s}\gamma^\mu P_L b|B(p)\rangle = D_{K^*}(k^2)W_\nu\left(\mathcal{X}_0 q^\mu q^\nu + \mathcal{X}_1\left(g^{\mu\nu} - \frac{q^\mu q^\nu}{q^2}\right) + \mathcal{X}_2\left(k^\mu - \frac{k.q}{q^2}q^\mu\right)q^\nu + i\mathcal{X}_3\epsilon^{\mu\nu\rho\sigma}k_\rho q_\sigma\right), \tag{5}$$

$$\langle[K(k_1)\pi(k_2)]_{K^*}|i\bar{s}\sigma^{\mu\nu}q_\nu P_{R,L}b|B(p)\rangle = D_{K^*}(k^2)W_\nu\left(\pm\mathcal{Y}_1\left(g^{\mu\nu} - \frac{q^\mu q^\nu}{q^2}\right) \pm \mathcal{Y}_2\left(k^\mu - \frac{k.q}{q^2}q^\mu\right)q^\nu + i\mathcal{Y}_3\epsilon^{\mu\nu\rho\sigma}k_\rho q_\sigma\right), \tag{6}$$

where, the subscript K^* in $[K(k_1)\pi(k_2)]_{K^*}$ indicates that the final sate is produced by the decay of a K^*, $D_{K^*}(k^2)$ is the K^* propagator, so that

$$|D_{K^*}(k^2)|^2 = \frac{g_{K^*K\pi}^2}{(k^2 - m_{K^*}^2)^2 + (m_{K^*}\Gamma_{K^*})^2}, \tag{7}$$

with $g_{K^*K\pi}$ being the $K^*K\pi$ coupling and the other parameters introduced are

$$W_\nu = K_\nu - \xi k_\nu, \quad K = k_1 - k_2, \quad k = k_1 + k_2, \quad \xi = \frac{k_1^2 - k_2^2}{k^2}.$$

The most general expression for the hadronic matrix element $\mathcal{H}_i^\mu$ can also be written using Lorentz invariance.

Since this hadronic matrix element arises from nonlocal contributions at the quark level, it involves introducing "new" form factors $\mathcal{Z}_1^i$, $\mathcal{Z}_2^i$ and $\mathcal{Z}_3^i$ corresponding to nonfactorizable contribution from each $\mathcal{H}_i^\mu$ in analogy with those introduced in Eq. (3) as follows:

$$\begin{aligned}\mathcal{H}_i^\mu &= \langle K^*(\epsilon^*,k)|i\int d^4x e^{iq\cdot x}T\{j_{em}^\mu(x),\mathcal{O}_i(0)\}|\bar{B}(p)\rangle \\ &= \epsilon_\nu^*\left(\mathcal{Z}_1^i\left(g^{\mu\nu}-\frac{q^\mu q^\nu}{q^2}\right)+\mathcal{Z}_2^i\left(k^\mu-\frac{k.q}{q^2}q^\mu\right)q^\nu+i\mathcal{Z}_3^i\epsilon^{\mu\nu\rho\sigma}k_\rho q_\sigma\right).\end{aligned} \tag{8}$$

Our definition follows Ref. [6] of "nonfactorizable" and includes those corrections that are not contained in the definition of form factors introduced in Eqs. (3) and (4). Here the most general form of $\mathcal{H}_i^\mu$ is written to ensure the conservation of EM current i.e., $q_\mu\mathcal{H}_i^\mu=0$.

The nonlocal effects represented by $\mathcal{H}_i^\mu$ can be taken into account by absorbing the contributions into redefined $\hat{C}_9$ and modifying the contribution from the electromagnetic dipole operator $\mathcal{O}_7$. The electromagnetic corrections to operators $\mathcal{O}_{1\text{–}6,8}$ can also contribute to $B\to K^*\gamma$ at $q^2=0$. Since, only the Wilson coefficient $\hat{C}_7$ contributes to $B\to K^*\gamma$, the charm loops at $q^2=0$ must contribute to $\hat{C}_7$ in order for the Wilson coefficient to be process independent. It is easily seen that the effect of this is to modify the $\hat{C}_7\langle K\pi|\bar{s}i\sigma^{\mu\nu}q_\nu(m_bP_R+m_sP_L)b|\bar{B}\rangle$ terms such that the form factors and Wilson coefficients mix in an essentially inseparable fashion. This holds true even for the leading logarithmic contributions [6,18]. Both factorizable and nonfactorizable contributions arising from electromagnetic corrections to hadronic operators up to all orders can in principle be included in this approach. The remaining contributions can easily be absorbed into a redefined "effective" Wilson coefficient $\hat{C}_9$ defined such that

$$\hat{C}_9\to\tilde{C}_9^{(j)}=\hat{C}_9+\Delta C_9^{(\text{fac})}(q^2)+\Delta C_9^{(j),(\text{non-fac})}(q^2) \tag{9}$$

where, $j=1,2,3$ and $\Delta C_9^{(\text{fac})}(q^2)$, $\Delta C_9^{(\text{non-fac})}(q^2)$ correspond to factorizable and soft gluon nonfactorizable contributions. Note that the nonfactorizable contributions necessitates the introduction of new form factors $\mathcal{Z}_j$ and the explicit dependence on $\mathcal{Z}_j/\mathcal{X}_j$ is absorbed in defining

$$\Delta C_9^{(\text{fac})}+\Delta C_9^{(j),(\text{non-fac})}=-\frac{16\pi^2}{q^2}\sum_{i=\{1\text{–}6,8\}}\hat{C}_i\frac{\mathcal{Z}_j^i}{\mathcal{X}_j}, \tag{10}$$

resulting in the j dependence of the term as indicated. We also mention that there is no nonfactorizable correction term in Eq. (8) analogous to $\mathcal{X}_0$ [in Eq. (3)] due EM current conservation as discussed above.

The corresponding corrections to $\hat{C}_7$ are taken into by the replacement,

$$\frac{2(m_b+m_s)}{q^2}\hat{C}_7\mathcal{Y}_j\to\tilde{\mathcal{Y}}_j=\frac{2(m_b+m_s)}{q^2}\hat{C}_7\mathcal{Y}_j+\cdots, \tag{11}$$

where the dots indicate other factorizable and nonfactorizable contributions and the factor $2(m_b+m_s)/q^2$ has been absorbed in the form factors $\tilde{\mathcal{Y}}_j$. Note that the $\tilde{\mathcal{Y}}_j$'s are in general complex because of the nonfactorizable contributions to the Wilson coefficient $\hat{C}_7$, but on-shell quarks and resonances do not contribute to them. It should be noted that $\tilde{C}_9^{(j)}$ includes contributions from both factorizable and nonfactorizable effects, whereas $\hat{C}_{10}$ is unaffected by strong interaction effects coming from electromagnetic corrections to hadronic operators. The use of a "wide tilde" versus "wide hat" throughout the paper is also meant as a notation to indicate this fact. It should be noted that $\hat{C}_{10}$ is real in the SM, whereas, $\tilde{C}_9^{(j)}$ and $\tilde{\mathcal{Y}}_j$ are in general complex within the SM. The amplitude in Eq. (2) can therefore be written as

$$\begin{aligned}&A(B(p)\to[K(k_1)\pi(k_2)]_{K^*}\ell^+\ell^-) \\ &\quad=\frac{G_F\alpha}{\sqrt{2}\pi}V_{tb}V_{ts}^*D_{K^*}(k^2) \\ &\quad\times\Bigg[\Bigg\{\left(C_LW.q\mathcal{X}_0q^\mu+C_L^{(1)}\mathcal{X}_1\left(K^\mu-\frac{W.q}{q^2}q^\mu-\xi k^\mu\right)+C_L^{(2)}W.q\mathcal{X}_2\left(k^\mu-\frac{k.q}{q^2}q^\mu\right)+iC_L^{(3)}\mathcal{X}_3\epsilon^{\mu\nu\rho\sigma}K_\nu k_\rho q_\sigma\right) \\ &\quad-\left(\zeta\tilde{\mathcal{Y}}_1\left(K^\mu-\frac{W.q}{q^2}q^\mu-\xi k^\mu\right)+\zeta W.q\tilde{\mathcal{Y}}_2\left(k^\mu-\frac{k.q}{q^2}q^\mu\right)+i\tilde{\mathcal{Y}}_3\epsilon^{\mu\nu\rho\sigma}K_\nu k_\rho q_\sigma\right)\Bigg\}\bar{\ell}\gamma_\mu P_L\ell+L\to R\Bigg],\end{aligned} \tag{12}$$

where, $C_{L,R} = \hat{C}_9 \mp \hat{C}_{10}$, $C^{(j)}_{L,R} = \tilde{C}^{(j)}_9 \mp \hat{C}_{10}$ and $\zeta = (m_b - m_s)/(m_b + m_s)$. It may be noted that no assumptions are made in obtaining Eq. (12) from Eq. (2). The form factors defined are not limited by power corrections in HQET [19]. We emphasize that Eq. (12) continues to be notionally exact. In our approach we will relate observables, hence, we do not need to evaluate the Wilson coefficients and form factors. Only in doing so approximations need to be made. In Appendix B comparative relation between the amplitude in Eq. (12) and the leading order expression excluding nonfactorization contribution used widely in literature are presented. These approximations are unnecessary for the discussions in this paper and are presented only as clarification of our notation and as ready reference for readers wanting to examine Eq. (12) in limiting conditions.

III. ANGULAR DISTRIBUTION AND OBSERVABLES

The decay $\bar{B}(p) \to K^*(k)\ell^+(q_1)\ell^-(q_2)$, with $K^*(k) \to K(k_1)\pi(k_2)$ on the mass shell, is completely describe by four independent kinematic variables. These kinematic variables are the lepton-pair invariant mass squared $q^2 = (q_1 + q_2)^2$, and the three angles ϕ, θ_ℓ and θ_K. The angle ϕ is the angle between the decay planes formed by $\ell^+\ell^-$ and $K\pi$. The angles θ_ℓ and θ_K are defined as follows: assuming that the K^* has a momentum along the positive z direction in B rest frame, θ_K is the angle between the K and the $+z$ axis and θ_ℓ is the angle of the ℓ^- with the $+z$ axis. The differential decay distribution of $B \to K^*\ell^+\ell^-$ is written as

$$\begin{aligned}\frac{d^4\Gamma(B \to K^*\ell^+\ell^-)}{dq^2 d\cos\theta_\ell d\cos\theta_K d\phi} &= I(q^2, \theta_\ell, \theta_K, \phi) \\ &= \frac{9}{32\pi}[I^s_1 \sin^2\theta_K + I^c_1 \cos^2\theta_K + (I^s_2 \sin^2\theta_K + I^c_2 \cos^2\theta_K)\cos 2\theta_\ell + I_3 \sin^2\theta_K \sin^2\theta_\ell \cos 2\phi \\ &\quad + I_4 \sin 2\theta_K \sin 2\theta_\ell \cos\phi + I_5 \sin 2\theta_K \sin\theta_\ell \cos\phi + I^s_6 \sin^2\theta_K \cos\theta_\ell \\ &\quad + I_7 \sin 2\theta_K \sin\theta_\ell \sin\phi + I_8 \sin 2\theta_K \sin 2\theta_\ell \sin\phi + I_9 \sin^2\theta_K \sin^2\theta_\ell \sin 2\phi]. \end{aligned} \tag{13}$$

The angular coefficients I's, which can be measured from the study of the angular distribution, are q^2 dependent. But for convenience we will suppress the explicit q^2 dependence.

The I's are conveniently expressed in terms of "seven" amplitudes. These comprise the six transversity amplitudes that survive in the massless lepton limit and an amplitude $\mathcal{A}_t$ that contributes only if the mass m of the lepton is finite. The six transversity amplitudes $\mathcal{A}^{L,R}_{\perp,\parallel,0}$, where $\perp$, $\parallel$ and 0 represent the polarizations of the on-shell K^* and L, R denote the chirality of the lepton current. The explicit expression for I's in terms of the transversity amplitudes $\mathcal{A}^{L,R}_{\perp,\parallel,0}$ and $\mathcal{A}_t$ are

$$I^s_1 = \frac{(2+\beta^2)}{4}[|\mathcal{A}^L_\perp|^2 + |\mathcal{A}^L_\parallel|^2 + (L \to R)] + \frac{4m^2}{q^2}\mathrm{Re}(\mathcal{A}^L_\perp \mathcal{A}^{R*}_\perp + \mathcal{A}^L_\parallel \mathcal{A}^{R*}_\parallel), \tag{14a}$$

$$I^c_1 = |\mathcal{A}^L_0|^2 + |\mathcal{A}^R_0|^2 + \frac{4m^2}{q^2}[|\mathcal{A}_t|^2 + 2\mathrm{Re}(\mathcal{A}^L_0 \mathcal{A}^{R*}_0)], \tag{14b}$$

$$I^s_2 = \frac{\beta^2}{4}[|\mathcal{A}^L_\perp|^2 + |\mathcal{A}^L_\parallel|^2 + (L \to R)], \tag{14c}$$

$$I^c_2 = -\beta^2[|\mathcal{A}^L_0|^2 + (L \to R)], \tag{14d}$$

$$I_3 = \frac{\beta^2}{2}[|\mathcal{A}^L_\perp|^2 - |\mathcal{A}^L_\parallel|^2 + (L \to R)], \tag{14e}$$

$$I_4 = \frac{\beta^2}{\sqrt{2}}[\mathrm{Re}(\mathcal{A}^L_0 \mathcal{A}^{L*}_\parallel) + (L \to R)], \tag{14f}$$

$$I_5 = \sqrt{2}\beta[\mathrm{Re}(\mathcal{A}^L_0 \mathcal{A}^{L*}_\perp) - (L \to R)], \tag{14g}$$

$$I^s_6 = 2\beta[\mathrm{Re}(\mathcal{A}^L_\parallel \mathcal{A}^{L*}_\perp) - (L \to R)], \tag{14h}$$

$$I_7 = \sqrt{2}\beta[\mathrm{Im}(\mathcal{A}^L_0 \mathcal{A}^{L*}_\parallel) - (L \to R)], \tag{14i}$$

$$I_8 = \frac{1}{\sqrt{2}}\beta^2[\mathrm{Im}(\mathcal{A}^L_0 \mathcal{A}^{L*}_\perp) + (L \to R)], \tag{14j}$$

$$I_9 = \beta^2[\mathrm{Im}(\mathcal{A}^{L*}_\parallel \mathcal{A}^L_\perp) + (L \to R)], \tag{14k}$$

where

$$\beta = \sqrt{1 - \frac{4m^2}{q^2}}.$$

We have dropped the explicit q^2 dependence of the transversity amplitudes $\mathcal{A}^{L,R}_{\perp,\parallel,0}$ and $\mathcal{A}_t$ for notational simplicity.

The seven amplitudes can be written in terms of the form factors $\mathcal{X}_{0,1,2,3}$ and $\mathcal{Y}_{1,2,3}$ as follows:

$$\mathcal{A}^{L,R}_\perp = N\sqrt{2}\lambda^{\frac{1}{2}}(m^2_B, m^2_{K^*}, q^2)[(\tilde{C}^{(3)}_9 \mp \hat{C}_{10})\mathcal{X}_3 - \tilde{\mathcal{Y}}_3], \tag{15a}$$

$$\mathcal{A}_{\parallel}^{L,R} = 2\sqrt{2}N[(\tilde{C}_9^{(1)} \mp \hat{C}_{10})\mathcal{X}_1 - \zeta\tilde{\mathcal{Y}}_1], \tag{15b}$$

$$\begin{aligned}\mathcal{A}_0^{L,R} = \frac{N}{2m_{K^*}\sqrt{q^2}}[(\tilde{C}_9^{(2)}\kappa \mp \hat{C}_{10})\{4k.q\mathcal{X}_1 \\ + \lambda(m_B^2, m_{K^*}^2, q^2)\mathcal{X}_2\} \\ - \zeta\{4k.q\tilde{\mathcal{Y}}_1 + \lambda(m_B^2, m_{K^*}^2, q^2)\tilde{\mathcal{Y}}_2\}],\end{aligned} \tag{15c}$$

$$\mathcal{A}_t = -\frac{N}{m_K^*}\sqrt{q^2}\lambda^{1/2}(m_B^2, m_{K^*}^2, q^2)\hat{C}_{10}\mathcal{X}_0, \tag{15d}$$

where,

$$\kappa = 1 + \frac{\tilde{C}_9^{(1)} - \hat{C}_9^{(2)}}{\hat{C}_9^{(2)}}\frac{4k.q\mathcal{X}_1}{4k.q\mathcal{X}_1 + \lambda(m_B^2, m_{K^*}^2, q^2)\mathcal{X}_2},$$

$\lambda(a,b,c) \equiv a^2 + b^2 + c^2 - 2(ab + bc + ac)$ and N is the normalization constant. In the narrow width approximation for the K^*, $|D_{K^*}(k^2)|^2$ simplifies to

$$|D_{K^*}(k^2)|^2 = \frac{48\pi^2 m_{K^*}^4}{\lambda^{3/2}(m_{K^*}^2, m_K^2, m_\pi^2)}\delta(k^2 - m_{K^*}^2). \tag{16}$$

This results in simplifying N to

$$N = V_{tb}V_{ts}^*\left[\frac{G_F^2\alpha^2}{3\times 2^{10}\pi^5 m_B^3}q^2\sqrt{\lambda(m_B^2, m_{K^*}^2, q^2)}\beta\right]^{1/2}.$$

We note that in principle the effect of finite K^* resonance width can easily be taken into account, however, we make no attempt to do so as the value of the normalization constant is not going to be used anywhere in our calculation.

The six transversity amplitudes described by Eqs. (15a)–(15c) which survive in the massless lepton case can be rewritten in a short-form notation by introducing new form factors $\mathcal{F}_\lambda$ and $\tilde{\mathcal{G}}_\lambda$ as follows:

$$\mathcal{A}_\lambda^{L,R} = C_{L,R}^\lambda\mathcal{F}_\lambda - \tilde{\mathcal{G}}_\lambda = (\tilde{C}_9^\lambda \mp \hat{C}_{10})\mathcal{F}_\lambda - \tilde{\mathcal{G}}_\lambda. \tag{17}$$

The expressions of $\mathcal{F}_\lambda$ and $\tilde{\mathcal{G}}_\lambda$ can be obtained by comparing Eq. (17) with Eqs. (15a)–(15c) and are given in Appendix (B). $\mathcal{F}_\lambda$ and $\tilde{\mathcal{G}}_\lambda$ are q^2 dependent form factors, suitably defined to include both factorizable and nonfactorizable corrections to all orders [2]. The form-factor dependence of $\tilde{C}_9^{(j)}$ indicated by "j" in Eqs. (15a)–(15c) is now translated to an effective helicity "λ" dependence of Wilson coefficient $\tilde{C}_9^\lambda$ as

$$\tilde{C}_9^\perp \equiv \tilde{C}_9^{(3)}, \qquad \tilde{C}_9^\parallel \equiv \tilde{C}_9^{(1)}, \qquad \tilde{C}_9^0 \equiv \tilde{C}_9^{(2)}\kappa. \tag{18}$$

It is easily seen that $\mathcal{F}_\lambda$ and $\tilde{\mathcal{G}}_\lambda$ are proportional to $\mathcal{X}_j$ and $\tilde{\mathcal{Y}}_j$ respectively. Thus $\mathcal{F}_\lambda$'s are completely real and $\tilde{\mathcal{G}}_\lambda$'s are complex in SM. All imaginary contributions to the amplitude arise from the complex $\tilde{C}_9^\lambda$ and $\tilde{\mathcal{G}}_\lambda$. An interesting observation is that $\mathcal{A}_\lambda^{L,R}$ remains unchanged if the nonfactorizable contributions between $\tilde{\mathcal{G}}_\lambda$ and $\tilde{C}_9^\lambda$ are rearranged. This observation differs from the conclusion obtained in Ref. [2] because $\tilde{C}_9^\lambda$ are now helicity dependent and implies that $\tilde{\mathcal{G}}_\lambda$ and $\tilde{C}_9^\lambda$ cannot be individually extracted.

Using very general arguments it is easy to see that the form of the amplitude described in Eq. (17) is the most general possible and the full decay amplitude can be completely described by them for the massless case. The amplitude must be described by the helicity of the K^* and can be divided into two parts, one that depends on the chirality of the lepton and another that does not. It is easily noted that the term described by $\mathcal{F}_\lambda$ is chirality dependent whereas the contribution corresponding to the effective photon vertex $\tilde{\mathcal{G}}_\lambda$ is not. The form factors $\mathcal{F}_\lambda$ and $\tilde{\mathcal{G}}_\lambda$ depend only on the helicity and the chirality dependence is absorbed completely into the Wilson coefficients. The coefficient of chirality dependent terms proportional to $\mathcal{F}_\lambda$ can themselves either depend on helicity or be independent of it. Hence, the amplitudes in Eq. (17) are parametrized in terms of three terms. Throughout the rest of the paper we will use only the form of the amplitudes in Eq. (17), which is the most general possible in the SM.

It is obvious from Eq. (13) that a complete study of the angular distribution involves eleven orthogonal terms allowing us to measure "eleven" observables. In the limit of massless lepton there exist two relations between the coefficient I's, i.e. $I_1^c = -I_2^c$ and $I_1^s = 3I_2^s$. This reduces the number of independent observables to "nine." We will divide our discussion into two parts. In Sec. IV we will restrict our discussion by assuming that the lepton is massless and in Sec. V we will generalize the discussion to the massive lepton case. In a previous paper [2] the mode $B \to K^*\ell^+\ell^-$ was studied in the limit of massless lepton and under the assumption of vanishing CP violation and absence of resonance contributions in the q^2 domains considered. Under these approximations $I_{7,8,9} = 0$ and the number of useful observables reduce to only "six." In this paper we carefully examine each of these assumptions and in particular take into account resonance contributions and the effect of massless lepton. As emphasized in Sec. II we have taken into account charm loop effects. The charm loop effect and other resonance contributions can make the amplitude complex. In the discussions that ensue we will assume that the amplitude is complex and ensure that all SM contributions, both factorizable and nonfactorizable, are taken into account completely when writing the most general parametrized amplitude.

Within SM, CP violation is expected to be extremely tiny and essentially unobservable [1,3] at the current level of experimental accuracy. In Ref. [1] the CP violating asymmetry was evaluated to be $\sim 3\times 10^{-4}$. This would

imply that one need at the very least 10^7 reconstructed events in this decay channel to observe the asymmetry at 1σ. Given this we have justifiably ignored CP violation in this channel and any observation of CP violation at the current level of experimental sensitivity would constitute an unambiguous signal of NP. In view of this, we ignore CP violation hence forth. It may be noted that CP violation can be easily included in our approach. However, we ignore it because it is not central to our discussion and we do not wish to complicate our notation accounting for unobservable effects within the SM. Under the assumption of vanishing CP violation the conjugate mode $\bar{B}\to\bar{K}^*\ell^+\ell^-$ has an identical decay distribution except that $I_{5,6,8,9}$ switch signs to become $-I_{5,6,8,9}$ in the differential decay distribution [1,3].

Integration over $\cos\theta_K$, $\cos\theta_\ell$ and ϕ results in the differential decay rate with respect to the invariant lepton mass:

$$\frac{d\Gamma}{dq^2}=\sum_{\lambda=0,\parallel,\perp}(|\mathcal{A}_\lambda^L|^2+|\mathcal{A}_\lambda^R|^2). \tag{19}$$

We define the relevant observables to be the three helicity fractions defined as

$$F_L=\frac{|\mathcal{A}_0^L|^2+|\mathcal{A}_0^R|^2}{\Gamma_f}, \tag{20a}$$

$$F_\parallel=\frac{|\mathcal{A}_\parallel^L|^2+|\mathcal{A}_\parallel^R|^2}{\Gamma_f}, \tag{20b}$$

$$F_\perp=\frac{|\mathcal{A}_\perp^L|^2+|\mathcal{A}_\perp^R|^2}{\Gamma_f}, \tag{20c}$$

where $\Gamma_f\equiv\sum_\lambda(|\mathcal{A}_\lambda^L|^2+|\mathcal{A}_\lambda^R|^2)$ and $F_L+F_\parallel+F_\perp=1$. The other observables are the six asymmetries defined below. The well-known forward-backward asymmetry $A_{\rm FB}$ is defined conventionally as

$$A_{\rm FB}=\frac{[\int_0^1-\int_{-1}^0]d\cos\theta_\ell\frac{d^2(\Gamma-\bar{\Gamma})}{dq^2d\cos\theta_\ell}}{\int_{-1}^1 d\cos\theta_\ell\frac{d^2(\Gamma+\bar{\Gamma})}{dq^2d\cos\theta_\ell}}, \tag{21}$$

and isolates the contribution from the I_6 term in Eq. (13).

Contributions from I_4 and I_5 in Eq. (13) are extracted by the two angular asymmetries,

$$A_4=\frac{[\int_{-\pi/2}^{\pi/2}-\int_{\pi/2}^{3\pi/2}]d\phi[\int_0^1-\int_{-1}^0]d\cos\theta_K[\int_0^1-\int_{-1}^0]d\cos\theta_\ell\frac{d^4(\Gamma+\bar{\Gamma})}{dq^2d\cos\theta_\ell d\cos\theta_K d\phi}}{\int_0^{2\pi}d\phi\int_{-1}^1 d\cos\theta_K\int_{-1}^1 d\cos\theta_\ell\frac{d^4(\Gamma+\bar{\Gamma})}{dq^2d\cos\theta_\ell d\cos\theta_K d\phi}}, \tag{22}$$

$$A_5=\frac{[\int_{-\pi/2}^{\pi/2}-\int_{\pi/2}^{3\pi/2}]d\phi[\int_0^1-\int_{-1}^0]d\cos\theta_K\int_{-1}^1 d\cos\theta_\ell\frac{d^4(\Gamma-\bar{\Gamma})}{dq^2d\cos\theta_\ell d\cos\theta_K d\phi}}{\int_0^{2\pi}d\phi\int_{-1}^1 d\cos\theta_K\int_{-1}^1 d\cos\theta_\ell\frac{d^4(\Gamma+\bar{\Gamma})}{dq^2d\cos\theta_\ell d\cos\theta_K d\phi}}. \tag{23}$$

The three new observables not considered in Ref. [2] are A_7, A_8 and A_9. These are nonzero if the amplitude is complex. They may be described in analogy as

$$A_7=\frac{[\int_0^{\pi}-\int_{\pi}^{2\pi}]d\phi[\int_0^1-\int_{-1}^0]d\cos\theta_K\int_{-1}^1 d\cos\theta_\ell\frac{d^4(\Gamma+\bar{\Gamma})}{dq^2d\cos\theta_\ell d\cos\theta_K d\phi}}{\int_0^{2\pi}d\phi\int_{-1}^1 d\cos\theta_K\int_{-1}^1 d\cos\theta_\ell\frac{d^4(\Gamma+\bar{\Gamma})}{dq^2d\cos\theta_\ell d\cos\theta_K d\phi}}, \tag{24}$$

$$A_8=\frac{[\int_0^{\pi}-\int_{\pi}^{2\pi}]d\phi[\int_0^1-\int_{-1}^0]d\cos\theta_K[\int_0^1-\int_{-1}^0]d\cos\theta_\ell\frac{d^4(\Gamma-\bar{\Gamma})}{dq^2d\cos\theta_\ell d\cos\theta_K d\phi}}{\int_0^{2\pi}d\phi\int_{-1}^1 d\cos\theta_K\int_{-1}^1 d\cos\theta_\ell\frac{d^4(\Gamma+\bar{\Gamma})}{dq^2d\cos\theta_\ell d\cos\theta_K d\phi}}, \tag{25}$$

$$A_9=\frac{[\int_0^{\pi/2}-\int_{\pi/2}^{\pi}+\int_0^{\pi}-\int_{3\pi/2}^{2\pi}]d\phi[\int_{-1}^1 d\cos\theta_K][\int_{-1}^1 d\cos\theta_\ell]\frac{d^4(\Gamma-\bar{\Gamma})}{dq^2d\cos\theta_\ell d\cos\theta_K d\phi}}{\int_0^{2\pi}d\phi\int_{-1}^1 d\cos\theta_K\int_{-1}^1 d\cos\theta_\ell\frac{d^4(\Gamma+\bar{\Gamma})}{dq^2d\cos\theta_\ell d\cos\theta_K d\phi}}. \tag{26}$$

The well-known forward-backward asymmetry $A_{\rm FB}$ and the five other angular asymmetries, A_4, A_5, A_7, A_8 and A_9 can be written directly in terms of the transversity amplitudes as follows:

$$A_{FB} = \frac{3}{2}\frac{\mathrm{Re}(\mathcal{A}_\parallel^L \mathcal{A}_\perp^{L^*} - \mathcal{A}_\parallel^R \mathcal{A}_\perp^{R^*})}{\Gamma_f}, \tag{27}$$

$$A_4 = \frac{\sqrt{2}}{\pi}\frac{\mathrm{Re}(\mathcal{A}_0^L \mathcal{A}_\parallel^{L^*} + \mathcal{A}_0^R \mathcal{A}_\parallel^{R^*})}{\Gamma_f}, \tag{28}$$

$$A_5 = \frac{3}{2\sqrt{2}}\frac{\mathrm{Re}(\mathcal{A}_0^L \mathcal{A}_\perp^{L^*} - \mathcal{A}_0^R \mathcal{A}_\perp^{R^*})}{\Gamma_f}, \tag{29}$$

$$A_7 = \frac{3}{2\sqrt{2}}\frac{\mathrm{Im}(\mathcal{A}_0^L \mathcal{A}_\parallel^{L*} - \mathcal{A}_0^R \mathcal{A}_\parallel^{R*})}{\Gamma_f}, \tag{30}$$

$$A_8 = \frac{\sqrt{2}}{\pi}\frac{\mathrm{Im}(\mathcal{A}_0^L \mathcal{A}_\perp^{L*} + \mathcal{A}_0^R \mathcal{A}_\perp^{R*})}{\Gamma_f}, \tag{31}$$

$$A_9 = \frac{3}{2\pi}\frac{\mathrm{Im}(\mathcal{A}_\parallel^{L*} \mathcal{A}_\perp^{L} + \mathcal{A}_\parallel^{R*} \mathcal{A}_\perp^{R})}{\Gamma_f}. \tag{32}$$

The observables A_4, A_5, $A_{\rm FB}$, A_7, A_8 and A_9 are related to the CP averaged observables S_4, S_5, $A_{\rm FB}^{\rm LHC}$, S_7, S_8 and S_9 measured by LHCb [5] as follows respectively,

$$A_4 = -\frac{2}{\pi}S_4, \qquad A_5 = \frac{3}{4}S_5, \qquad A_{\rm FB} = -A_{\rm FB}^{\rm LHC}, \\ A_7 = \frac{3}{4}S_7, \qquad A_8 = -\frac{2}{\pi}S_8, \qquad A_9 = \frac{3}{2\pi}S_9. \tag{33}$$

We emphasize that our observables $A_{4,5,7,8,9}$ are CP conserving asymmetries and in particular A_9 and should not be confused with the CP violating asymmetry measured by LHCb [5] also denoted by A_9. In our notation we would refer to the CP violating asymmetries as $A_{4,5,6,7,8,9}^{CP}$. The observables F_L and $A_{\rm FB}$ have been measured by different experiments *BABAR*, Belle, CDF and LHCb [5,20–26]. By doing an angular analysis in the angle ϕ, LHCb has measured the observable S_3 [5]. S_3 is related to the transversity helicity fraction $F_\perp$ through the relation

$$S_3 = -\frac{1 - F_L - 2F_\perp}{2}. \tag{34}$$

The observables F_L, $F_\perp$, A_4, A_5, $A_{\rm FB}$, A_7, A_8 and A_9 defined in this section are not independent. In the subsequent sections we explore the relation between them.

IV. THE MASSLESS LEPTON LIMIT

In this section we generalize the approach developed in Ref. [2] to include all contributions from the SM that were ignored as their effects are subdominant, except that we still restrict our discussion to the limit where the lepton is massless. The corrections arising from massive leptons will be taken into account later in Sec V. In particular we will consider the possibility that the amplitudes $\mathcal{A}_\lambda^{L,R}$ are in general complex. As already mentioned the imaginary contribution can be totally attributed to the complex $\tilde{C}_9^\lambda$ and $\tilde{\mathcal{G}}_\lambda$. This would include loop contributions that are both factorizable and nonfactorizable and all resonance contributions. We also take into account that the nonfactorizable contributions can introduce an "effective helicity (λ) dependence" in the Wilson coefficient $\tilde{C}_9^\lambda$.

In Ref. [2] a new variable r_λ was introduced that led to significant simplification. We once again introduce the same "real variable" r_λ defined as

$$r_\lambda = \frac{\mathrm{Re}(\tilde{\mathcal{G}}_\lambda)}{\mathcal{F}_\lambda} - \mathrm{Re}(\tilde{C}_9^\lambda). \tag{35}$$

Since, we now consider $\tilde{C}_9^\lambda$ and $\tilde{\mathcal{G}}_\lambda$ to be complex in general, we have modified r_λ to include only the real contributions i.e., $\mathrm{Re}(\tilde{C}_9^\lambda)$ and $\mathrm{Re}(\tilde{\mathcal{G}}_\lambda)$. The amplitude $\mathcal{A}_\lambda^{L,R}$ in Eq. (17) can thus be written as

$$\begin{aligned}\mathcal{A}_\lambda^{L,R} &= (\tilde{C}_9^\lambda \mp \hat{C}_{10})\mathcal{F}_\lambda - \tilde{\mathcal{G}}_\lambda \\ &= (\mp \hat{C}_{10} - r_\lambda)\mathcal{F}_\lambda + i\varepsilon_\lambda,\end{aligned} \tag{36}$$

where $\varepsilon_\lambda \equiv \mathrm{Im}(\tilde{C}_9^\lambda)\mathcal{F}_\lambda - \mathrm{Im}(\tilde{\mathcal{G}}_\lambda)$. The use of ε_λ is not necessarily meant to imply that the imaginary parts are negligibly small. We make no such assumption. It is, however, to be expected that the imaginary contributions are subdominant. The presence of the ε_λ term introduces three extra variables in comparison to the discussion in Ref. [2]. However, we now have three extra observables A_7, A_8 and A_9. Hence, dealing with complex amplitude introduces only a technical difficulty of solving for additional variables. We begin by expressing the observables F_L, $F_\parallel$, $F_\perp$, A_4, A_5, $A_{\rm FB}$, A_7, A_8 and A_9 in terms of $\hat{C}_{10}$, r_λ, $\mathcal{F}_\lambda$ and ε_λ as follows:

$$F_L\Gamma_f = 2\mathcal{F}_0^2(r_0^2 + \hat{C}_{10}^2) + 2\varepsilon_0^2, \tag{37}$$

$$F_\parallel\Gamma_f = 2\mathcal{F}_\parallel^2(r_\parallel^2 + \hat{C}_{10}^2) + 2\varepsilon_\parallel^2, \tag{38}$$

$$F_\perp\Gamma_f = 2\mathcal{F}_\perp^2(r_\perp^2 + \hat{C}_{10}^2) + 2\varepsilon_\perp^2, \tag{39}$$

$$\sqrt{2}\pi A_4\Gamma_f = 4\mathcal{F}_0\mathcal{F}_\parallel(r_0 r_\parallel + \hat{C}_{10}^2) + 4\varepsilon_0\varepsilon_\parallel, \tag{40}$$

$$\sqrt{2}A_5\Gamma_f = 3\mathcal{F}_0\mathcal{F}_\perp\hat{C}_{10}(r_0 + r_\perp), \tag{41}$$

$$A_{\rm FB}\Gamma_f = 3\mathcal{F}_\parallel\mathcal{F}_\perp\hat{C}_{10}(r_\parallel + r_\perp), \tag{42}$$

$$\sqrt{2}A_7\Gamma_f = 3\hat{C}_{10}(\mathcal{F}_0\varepsilon_\parallel - \mathcal{F}_\parallel\varepsilon_0), \tag{43}$$

$$\pi A_8\Gamma_f = 2\sqrt{2}(\mathcal{F}_0 r_0\varepsilon_\perp - \mathcal{F}_\perp r_\perp\varepsilon_0), \tag{44}$$

$$\pi A_9\Gamma_f = 3(\mathcal{F}_\perp r_\perp\varepsilon_\parallel - \mathcal{F}_\parallel r_\parallel\varepsilon_\perp). \tag{45}$$

One immediately concludes that

$$2\frac{\varepsilon_0^2}{\Gamma_f} \le F_L, \tag{46}$$

$$2\frac{\varepsilon_\parallel^2}{\Gamma_f} \le F_\parallel, \tag{47}$$

$$2\frac{\varepsilon_\perp^2}{\Gamma_f} \le F_\perp. \tag{48}$$

Equations (37)–(42) can be easily transformed to the form in Ref. [2] by the redefinition of the observables F_L, $F_\parallel$, $F_\perp$ and A_4 as

$$F'_\lambda = F_\lambda - \frac{2\varepsilon_\lambda^2}{\Gamma_f}, \tag{49}$$

$$A'_4 = A_4 - \frac{2\sqrt{2}\varepsilon_0\varepsilon_\parallel}{\pi\Gamma_f}. \tag{50}$$

It should be noted that $F'_L + F'_\parallel + F'_\perp \le 1$. Since only the ratios of the form factors $\mathcal{F}_\lambda$ play a role in the relations we wish to derive we define ratios of form factors P_1, P_2 and P_3:

$$\mathsf{P}_1 = \frac{\mathcal{F}_\perp}{\mathcal{F}_\parallel}, \tag{51}$$

$$\mathsf{P}_2 = \frac{\mathcal{F}_\perp}{\mathcal{F}_0}, \tag{52}$$

$$\mathsf{P}_3 = \frac{\mathcal{F}_\perp}{\mathcal{F}_0 + \mathcal{F}_\parallel} \equiv \frac{\mathsf{P}_1\mathsf{P}_2}{\mathsf{P}_1 + \mathsf{P}_2}. \tag{53}$$

Following these redefinitions Eqs. (37)–(42) can be recast into three sets of equations just as done in Ref. [2]. The three sets of equation are

(i) Set-I

$$F'_\parallel\Gamma_f = 2\frac{\mathcal{F}_\perp^2}{\mathsf{P}_1^2}(r_\parallel^2 + \hat{C}_{10}^2) \tag{54}$$

$$F'_\perp\Gamma_f = 2\mathcal{F}_\perp^2(r_\perp^2 + \hat{C}_{10}^2) \tag{55}$$

$$A_{\rm FB}\Gamma_f = 3\frac{\mathcal{F}_\perp^2}{\mathsf{P}_1}\hat{C}_{10}(r_\parallel + r_\perp) \tag{56}$$

(ii) Set-II

$$F'_L\Gamma_f = 2\frac{\mathcal{F}_\perp^2}{\mathsf{P}_2^2}(r_0^2 + \hat{C}_{10}^2) \tag{57}$$

$$F'_\perp\Gamma_f = 2\mathcal{F}_\perp^2(r_\perp^2 + \hat{C}_{10}^2) \tag{58}$$

$$\sqrt{2}A_5\Gamma_f = 3\frac{\mathcal{F}_\perp^2}{\mathsf{P}_2}\hat{C}_{10}(r_0 + r_\perp) \tag{59}$$

(iii) Set-III

$$(F'_L + F'_\parallel + \sqrt{2}\pi A'_4)\Gamma_f = 2\frac{\mathcal{F}_\perp^2}{\mathsf{P}_3^2}(r_\wedge^2 + \hat{C}_{10}^2) \tag{60}$$

$$F'_\perp\Gamma_f = 2\mathcal{F}_\perp^2(r_\perp^2 + \hat{C}_{10}^2) \tag{61}$$

$$(A_{\rm FB} + \sqrt{2}A_5)\Gamma_f = 3\frac{\mathcal{F}_\perp^2}{\mathsf{P}_3}\hat{C}_{10}(r_\wedge + r_\perp) \tag{62}$$

In the above we have defined $r_\wedge$ as

$$r_\wedge = \frac{r_\parallel\mathsf{P}_2 + r_0\mathsf{P}_1}{\mathsf{P}_2 + \mathsf{P}_1}. \tag{63}$$

Of the nine equations defined in the three sets only six of them are independent. These are the three equations, Eqs. (54)–(56) in Set-I, two equations (57) and (59) from Set-II and Eq. (60) of Set-III. It is easy to see that Set-II and Set-III can be obtained from Set-I by the following replacements:

(i) Set-II from Set-I
$F'_\parallel \to F'_L$, $A_{\rm FB} \to \sqrt{2}A_5$, $r_\parallel \to r_0$ and $\mathsf{P}_1 \to \mathsf{P}_2$ (or $\mathcal{F}_\parallel \to \mathcal{F}_0$).

(ii) Set-III from Set-I
$F'_\parallel \to F'_L + F'_\parallel + \sqrt{2}\pi A'_4$, $A_{\rm FB} \to A_{\rm FB} + \sqrt{2}A_5$, $r_\parallel \to r_\wedge$ and $\mathsf{P}_1 \to \mathsf{P}_3$ (or $\mathcal{F}_\parallel \to \mathcal{F}_\parallel + \mathcal{F}_0$).

It is obvious that we only need to solve Set-I to obtain $r_\parallel$ and $r_\perp$ in terms of P_1, $F'_\parallel$, $F'_\perp$ and $A_{\rm FB}$. The solutions to Set-II and Set-III can be obtained by simple replacements.

The solution of Set-I gives (from Appendix. A)

$$r_\parallel = \pm\frac{\sqrt{\Gamma_f}}{\sqrt{2}\mathcal{F}_\perp}\frac{(\mathsf{P}_1^2F'_\parallel + \frac{1}{2}\mathsf{P}_1Z'_1)}{\sqrt{\mathsf{P}_1^2F'_\parallel + F'_\perp + \mathsf{P}_1Z'_1}}, \tag{64}$$

$$r_\perp = \pm\frac{\sqrt{\Gamma_f}}{\sqrt{2}\mathcal{F}_\perp}\frac{(F'_\perp + \frac{1}{2}\mathsf{P}_1Z'_1)}{\sqrt{\mathsf{P}_1^2F'_\parallel + F'_\perp + \mathsf{P}_1Z'_1}}, \tag{65}$$

where Z'_1 is defined as

$$Z'_1 = \sqrt{4F'_{\parallel}F'_{\perp} - \frac{16}{9}A_{\rm FB}^2}. \tag{66}$$

The solution to Set-II is now easily seen to be

$$r_0 = \pm\frac{\sqrt{\Gamma_f}}{\sqrt{2}\mathcal{F}_\perp}\frac{(\mathsf{P}_2^2F'_L + \frac{1}{2}\mathsf{P}_2Z'_2)}{\sqrt{\mathsf{P}_2^2F'_L + F'_\perp + \mathsf{P}_2Z'_2}}, \tag{67}$$

$$r_\perp = \pm\frac{\sqrt{\Gamma_f}}{\sqrt{2}\mathcal{F}_\perp}\frac{(F'_\perp + \frac{1}{2}\mathsf{P}_2Z'_2)}{\sqrt{\mathsf{P}_2^2F'_L + F'_\perp + \mathsf{P}_2Z'_2}}, \tag{68}$$

with Z'_2 defined as

$$Z'_2 = \sqrt{4F'_LF'_\perp - \frac{32}{9}A_5^2}. \tag{69}$$

On comparing the solutions for $r_\perp$ in Eqs. (65) and (68) obtained from Set-I and Set-II respectively, we obtain a relation for P_2 in terms of P_1 and observables to be

$$\mathsf{P}_2 = \frac{2\mathsf{P}_1A_{\rm FB}F'_\perp}{s\sqrt{2}A_5(2F'_\perp + Z'_1\mathsf{P}_1) - Z'_2\mathsf{P}_1A_{\rm FB}}, \tag{70}$$

with $s \in \{-1, +1\}$. To remove the ambiguities in the P_2 solution let us divide Eq. (59) by Eq. (56) and using Eqs. (64)–(68) we get

$$\frac{\sqrt{2}A_5}{A_{\rm FB}} = \frac{\mathsf{P}_1}{\mathsf{P}_2}\frac{\sqrt{\mathsf{P}_2^2F'_L + F'_\perp + \mathsf{P}_2Z'_2}}{\sqrt{\mathsf{P}_1^2F'_\parallel + F'_\perp + \mathsf{P}_1Z'_1}} = \frac{\mathsf{P}_1}{\mathsf{P}_2}\frac{(2F'_\perp + \mathsf{P}_2Z'_2)}{(2F'_\perp + \mathsf{P}_1Z'_1)}. \tag{71}$$

Substituting it in Eq. (70) we have

$$s(2F'_\perp + \mathsf{P}_2Z'_2) - Z'_2\mathsf{P}_2 = 2F'_\perp,$$

which is valid for the whole q^2 region only for $s = 1$.

Finally we write the $r_\perp$ solution obtained from Set-III:

$$r_\perp = \pm\frac{\sqrt{\Gamma_f}}{\sqrt{2}\mathcal{F}_\perp}\frac{(F'_\perp + \frac{1}{2}\mathsf{P}_3Z'_3)}{\sqrt{\mathsf{P}_3^2(F'_\parallel + F'_L + \sqrt{2}\pi A'_4) + F'_\perp + \mathsf{P}_3Z'_3}}, \tag{72}$$

where Z'_3 is defined as

$$Z'_3 = \sqrt{4(F'_L + F'_\parallel + \sqrt{2}\pi A'_4)F'_\perp - \frac{16}{9}(A_{\rm FB} + \sqrt{2}A_5)^2}. \tag{73}$$

Analogous comparison of solutions for $r_\perp$ in Eqs. (65) and (72) obtained from Set-I and Set-III respectively, results in a relation for P_3 in terms of P_1:

$$\mathsf{P}_3 = \frac{2\mathsf{P}_1A_{\rm FB}F'_\perp}{(A_{\rm FB} + \sqrt{2}A_5)(2F'_\perp + Z'_1\mathsf{P}_1) - Z'_3\mathsf{P}_1A_{\rm FB}}. \tag{74}$$

The ambiguity in the P_3 solution is also taken to be positive for the same reason as the P_2 solution. The form-factor ratio P_3 is not however independent of P_1 and P_2 and is related by Eq. (53). Substituting Eqs. (70) and (74) in Eq. (53) we obtain the relation between the observables as

$$Z'_3 = Z'_1 + Z'_2. \tag{75}$$

The relations derived so far involve the primed observables that depend on $\varepsilon_\perp$, $\varepsilon_\parallel$ and ε_0. However, the ε_λ's can be solved using A_7, A_8 and A_9 from Eqs. (43)–(45) to give

$$\varepsilon_\perp = \frac{\sqrt{2}\pi\Gamma_f}{(r_0 - r_\parallel)\mathcal{F}_\perp}\left[\frac{A_9\mathsf{P}_1}{3\sqrt{2}} + \frac{A_8\mathsf{P}_2}{4} - \frac{A_7\mathsf{P}_1\mathsf{P}_2r_\perp}{3\pi\hat{C}_{10}}\right], \tag{76}$$

$$\varepsilon_\parallel = \frac{\sqrt{2}\pi\Gamma_f}{(r_0 - r_\parallel)\mathcal{F}_\perp}\left[\frac{A_9r_0}{3\sqrt{2}r_\perp} + \frac{A_8\mathsf{P}_2r_\parallel}{4\mathsf{P}_1r_\perp} - \frac{A_7\mathsf{P}_2r_\parallel}{3\pi\hat{C}_{10}}\right], \tag{77}$$

$$\varepsilon_0 = \frac{\sqrt{2}\pi\Gamma_f}{(r_0 - r_\parallel)\mathcal{F}_\perp}\left[\frac{A_9\mathsf{P}_1r_0}{3\sqrt{2}\mathsf{P}_2r_\perp} + \frac{A_8r_\parallel}{4r_\perp} - \frac{A_7\mathsf{P}_1r_0}{3\pi\hat{C}_{10}}\right]. \tag{78}$$

A point to be noted that the $(\varepsilon_\lambda/\Gamma_f^{\frac{1}{2}})$'s are free from the form factor $\mathcal{F}_\perp$ and Γ_f as can easily be seen from the expressions for $r_\parallel$, $r_\perp$ and r_0 [Eqs. (64), (65) and (67)], as well as $\hat{C}_{10}$ derived in Eq. (A12). Indeed, since P_2 can be expressed in terms P_1 and observables using Eq. (70), it is easy to see that *each of the ε_λ's are completely expressed in terms of observables and the form-factor ratio* P_1. However, these solutions are essentially iterative, since the r_λ's and $\hat{C}_{10}$ are derived in terms of the primed observables that depend on ε_λ. If the $(\varepsilon_\lambda/\Gamma_f^{\frac{1}{2}})$ are small as should be expected, accurate solutions for them can be found with a few iterations.

Solving for A_4 from Eq. (75) the relation among the observables is

$$A_4 = \frac{2\sqrt{2}\varepsilon_\parallel\varepsilon_0}{\pi\Gamma_f} + \frac{8A_5A_{\rm FB}}{9\pi(F_\perp - \frac{2\varepsilon_\perp^2}{\Gamma_f})} + \sqrt{2}\frac{\sqrt{(F_L - \frac{2\varepsilon_0^2}{\Gamma_f})(F_\perp - \frac{2\varepsilon_\perp^2}{\Gamma_f}) - \frac{8}{9}A_5^2}\sqrt{(F_\parallel - \frac{2\varepsilon_\parallel^2}{\Gamma_f})(F_\perp - \frac{2\varepsilon_\perp^2}{\Gamma_f}) - \frac{4}{9}A_{\rm FB}^2}}{\pi(F_\perp - \frac{2\varepsilon_\perp^2}{\Gamma_f})}. \tag{79}$$

This relation for A_4 in terms of other observables F_L, $F_\perp$, A_5, $A_{\rm FB}$, A_7, A_8 and A_9 is a generalization of the relation derived in Ref. [2]. A point to be noted is that while we have solved for the observable A_4, we could have used Eq. (75) to derive an expression for any of the other observable. However, only the solution for A_4 is unique and hence the one we consider. The validity of this relation is a test of the consistency of the values of all measured observables. Unlike the expression obtained in Ref. [2], we now have a relation between observables that depends on only one hadronic parameter, the ratio of form factors P_1. It is interesting to note that P_1 does not receive nonfactorizable contributions and is uncorrected by charm loop effects. Since, P_1 is independent of the universal wave functions [6,27] in HQET, it can be reliably calculated as an expansion in both the strong coupling constant α_s and $\Lambda_{\rm QCD}/m_b$. The dependence of A_4 on P_1 is rather weak, since the observables A_7, A_8 and A_9 are observed to be small and are currently consistent with zero as expected [5]. If A_7, A_8 and A_9 are all observed to be zero, it is easy to see from Eqs. (76)–(78) that $\varepsilon_\perp = \varepsilon_\parallel = \varepsilon_0 = 0$ reducing the relation in Eq. (79) to

$$A_4 = \frac{8A_5A_{\rm FB}}{9\pi F_\perp} + \sqrt{2}\frac{\sqrt{F_LF_\perp - \frac{8}{9}A_5^2}\sqrt{F_\parallel F_\perp - \frac{4}{9}A_{\rm FB}^2}}{\pi F_\perp} \tag{80}$$

which was derived in Ref. [2]. Interestingly, in the limit of vanishing imaginary contributions, A_4 can be expressed purely in terms of observables and is free from any form factor or their ratio. In Appendix B it is shown that both P_1 and P_2 are always negative. An interesting observation that $A_{\rm FB}$ and A_5 always have same signs can be then made from the relation in Eq. (71). Hence, we can arrive to a conclusion that, from Eq. (79) the observable A_4 is always positive unless the term proportional to $\varepsilon_\parallel\varepsilon_0$ is negative and it dominates over the rest of the terms in the expression.

A_4 is an observable and hence must always be real. This places constraints on the arguments of the radicals, which are directly related to the fact that Z_1', Z_2' and Z_3' are all real. The constraint that Z_1' is real in turn implies that

$$F_\parallel F_\perp - \frac{4}{9}A_{\rm FB}^2 \geq F_\parallel F_\perp\left(\frac{2\varepsilon_\parallel^2}{\Gamma_f F_\parallel} + \frac{2\varepsilon_\perp^2}{\Gamma_f F_\perp} - \frac{4\varepsilon_\parallel^2\varepsilon_\perp^2}{\Gamma_f^2 F_\parallel F_\perp}\right). \tag{81}$$

In Eqs. (46)–(48), we showed that $0 \leq \frac{2\varepsilon_\lambda^2}{\Gamma_f F_\lambda} \leq 1$, implying that the rhs of Eq. (81) must itself be greater than zero. This imposes the following constraint:

$$F_\parallel F_\perp - \frac{4}{9}A_{\rm FB}^2 \geq 0. \tag{82}$$

A similar constraint arising from Z_2' and Z_3' also being real implies that

$$F_LF_\perp - \tfrac{8}{9}A_5^2 \geq 0, \tag{83}$$

$$(F_L + F_\parallel + \sqrt{2}\pi A_4)F_\perp - \tfrac{4}{9}(A_{\rm FB} + \sqrt{2}A_5)^2 \geq 0. \tag{84}$$

The equality in the above three relations holds only when a minimum of two of the ε_λ's are zero. For example, $\varepsilon_\parallel$ and $\varepsilon_\perp$ are zero for the equality to hold in Eq. (82), whereas ε_0 and $\varepsilon_\perp$ are zero for Eq. (83). The three inequalities in Eqs. (82)–(84) impose constraints on the parameter space of observables. It is obvious that nonzero ε_λ's will in general restrict the parameter space of observables even further. We emphasize that this conclusion is valid without any exception. We will come back to this point in Sec. VII when we discuss the tests of the relation for A_4 in Eq. (79).

V. GENERALIZATION TO INCLUDE LEPTON MASSES

In this section we extend the model independent approach developed in the previous section (Sec. IV) to include the lepton mass m. One of the consequences of retaining the lepton mass is the need to include an additional amplitude in order to describe the full decay rate, since the term proportional to q_μ in the amplitude cannot be dropped for the massive lepton case (for a review [8]). In addition to the six amplitude $\mathcal{A}_\lambda^{L,R}$ where $\lambda \in \{0, \parallel, \perp\}$ the decay amplitude also depends on $\mathcal{A}_t$, resulting in a total of seven amplitudes. These amplitudes are given in Eqs. (15a)–(15d). In addition, since the massive leptons are no longer chirality eigenstates, terms involving admixtures of helicities that are proportional to m^2/q^2 [see Eqs. (14a) and (14b)] contribute to the differential decay rate.

These additional contributions complicate the extraction of the helicity amplitudes. The observables F_L, $F_\parallel$, $F_\perp$, A_4, A_5 and $A_{\rm FB}$ given in Sec. IV are modified because of the presence of the new transversity amplitude $\mathcal{A}_t$ and helicity admixture terms in the decay distribution. This in turn results in modifying the relations in Eqs. (79) and (80). The effect of the mass of the lepton is always included in the measured observables and it is not possible to measure any observable without the mass effects. In order to distinguish the "hypothetical observables without the mass effects" considered in Sec. IV from these true observables, we define them with a superscript "o" and relate to the massless limit observables as

$$\Gamma_f^{\rm o} = \beta^2\Gamma_f + 3\mathbb{T}_1, \tag{85a}$$

$$F_L^{\rm o} = \frac{1}{\Gamma_f^{\rm o}}(\beta^2\Gamma_f F_L + \mathbb{T}_1), \tag{85b}$$

$$F_{\parallel}^{o} = \frac{1}{\Gamma_f^o}(\beta^2\Gamma_f F_{\parallel} + \mathbb{T}_1), \tag{85c}$$

$$F_{\perp}^{o} = \frac{1}{\Gamma_f^o}(\beta^2\Gamma_f F_{\perp} + \mathbb{T}_1), \tag{85d}$$

$$A_4^o = \frac{\Gamma_f}{\Gamma_f^o}\beta^2 A_4, \tag{85e}$$

$$A_5^o = \frac{\Gamma_f}{\Gamma_f^o}\beta A_5, \tag{85f}$$

$$A_{FB}^o = \frac{\Gamma_f}{\Gamma_f^o}\beta A_{FB}, \tag{85g}$$

$$A_7^o = \frac{\Gamma_f}{\Gamma_f^o}\beta A_7, \tag{85h}$$

$$A_8^o = \frac{\Gamma_f}{\Gamma_f^o}\beta^2 A_8, \tag{85i}$$

$$A_9^o = \frac{\Gamma_f}{\Gamma_f^o}\beta^2 A_9. \tag{85j}$$

In the above we have defined

$$\mathbb{T}_1 = (1+E_1)\frac{m^2}{q^2}\Gamma_f \quad \text{where}$$

$$E_1 = \frac{|\mathcal{A}_t|^2}{\Gamma_f} + \frac{2}{\Gamma_f}\mathrm{Re}[\mathcal{A}_{\parallel}^L\mathcal{A}_{\parallel}^{R*} + \mathcal{A}_{\perp}^L\mathcal{A}_{\perp}^{R*} + \mathcal{A}_0^L\mathcal{A}_0^{R*}].$$

Using

$$2\mathrm{Re}[\mathcal{A}_\lambda^L\mathcal{A}_\lambda^{R*}] = |\mathcal{A}_\lambda^L + \mathcal{A}_\lambda^R|^2 - \Gamma_f F_\lambda$$

and the Cauchy-Schwarz inequality, we find

$$\mathbb{T}_1 = \left(|\mathcal{A}_t|^2 + \sum_{\lambda=\{\parallel,\perp,0\}}|\mathcal{A}_\lambda^L + \mathcal{A}_\lambda^R|^2\right)\frac{m^2}{q^2} \tag{86}$$

$$\leq (|\mathcal{A}_t|^2 + 2\Gamma_f)\frac{m^2}{q^2} \tag{87}$$

which is always positive and bounded. This bound is important since $\mathbb{T}_1$ has not been measured so far. $\mathbb{T}_1$ can also be expressed in terms of angular coefficients as

$$\frac{\mathbb{T}_1}{\Gamma_f^o} = \frac{1}{3} - \frac{4I_2^s - I_2^c}{3\Gamma_f^o} = \frac{1}{3} - \frac{16}{9}A_{10} + \frac{64}{27}A_{11} \tag{88}$$

and measured in terms of two new observables A_{10} and A_{11}, defined in terms of angular asymmetries as follows:

$$A_{10} = \frac{\int_0^{2\pi}d\phi\int_0^1 d\cos\theta_K[\int_{-1}^{-1/2} - \int_{-1/2}^{1/2} + \int_{1/2}^1]d\cos\theta_\ell \frac{d^4(\Gamma+\bar{\Gamma})}{dq^2 d\cos\theta_\ell d\cos\theta_K d\phi}}{\int_0^{2\pi}d\phi\int_{-1}^1 d\cos\theta_K\int_{-1}^1 d\cos\theta_\ell \frac{d^4(\Gamma+\bar{\Gamma})}{dq^2 d\cos\theta_\ell d\cos\theta_K d\phi}}, \tag{89}$$

$$A_{11} = \frac{\int_0^{2\pi}d\phi[\int_{-1}^{-1/2} - \int_{-1/2}^{1/2} + \int_{1/2}^1]d\cos\theta_K[\int_{-1}^{-1/2} - \int_{-1/2}^{1/2} + \int_{1/2}^1]d\cos\theta_\ell \frac{d^4(\Gamma+\bar{\Gamma})}{dq^2 d\cos\theta_\ell d\cos\theta_K d\phi}}{\int_0^{2\pi}d\phi\int_{-1}^1 d\cos\theta_K\int_{-1}^1 d\cos\theta_\ell \frac{d^4(\Gamma+\bar{\Gamma})}{dq^2 d\cos\theta_\ell d\cos\theta_K d\phi}}. \tag{90}$$

If the two asymmetries A_{10} and A_{11} are measured experimentally then we can get the estimate of the correction term arising due to lepton masses. However, from Eq. (86) it can be seen that $\mathbb{T}_1$ is proportional to lepton mass (square) m^2/q^2 which is very small and difficult to measure except at small q^2. In the limit of zero lepton mass $\mathbb{T}_1$ vanishes which gives a constraint on these two observables by

$$A_{10} - \frac{4}{3}A_{11} = \frac{3}{16}. \tag{91}$$

A deviation from this relation would indicate the effect of the nonzero lepton mass and provide an estimate of the size the mass corrections. The observables are reexpressed in terms of the variables r_λ [defined in Eq. (35)] as follows:

$$F_L^o\Gamma_f^o = 2\beta^2\frac{\mathcal{F}_\perp^2}{\mathsf{P}_2^2}(r_0^2 + \hat{C}_{10}^2) + 2\beta^2\varepsilon_0^2 + \mathbb{T}_1, \tag{92}$$

$$F_\parallel^o\Gamma_f^o = 2\beta^2\frac{\mathcal{F}_\perp^2}{\mathsf{P}_1^2}(r_\parallel^2 + \hat{C}_{10}^2) + 2\beta^2\varepsilon_\parallel^2 + \mathbb{T}_1, \tag{93}$$

$$F_\perp^{\rm o}\Gamma_f^{\rm o} = 2\beta^2\mathcal{F}_\perp^2(r_\perp^2 + \hat{C}_{10}^2) + 2\beta^2\varepsilon_\perp^2 + \mathbb{T}_1, \quad (94)$$

$$\sqrt{2}\pi A_4^{\rm o}\Gamma_f^{\rm o} = 4\beta^2\frac{\mathcal{F}_\perp^2}{\mathsf{P}_1\mathsf{P}_2}(r_0 r_\parallel + \hat{C}_{10}^2) + 4\beta^2\varepsilon_0\varepsilon_\parallel, \quad (95)$$

$$\sqrt{2}A_5^{\rm o}\Gamma_f^{\rm o} = 3\beta\frac{\mathcal{F}_\perp^2}{\mathsf{P}_2}\hat{C}_{10}(r_0 + r_\perp), \quad (96)$$

$$A_{\rm FB}^{\rm o}\Gamma_f^{\rm o} = 3\beta\frac{\mathcal{F}_\perp^2}{\mathsf{P}_1}\hat{C}_{10}(r_\parallel + r_\perp), \quad (97)$$

$$\sqrt{2}A_7^{\rm o}\Gamma_f^{\rm o} = 3\beta\hat{C}_{10}(\mathcal{F}_0\varepsilon_\parallel - \mathcal{F}_\parallel\varepsilon_0), \quad (98)$$

$$\pi A_8^{\rm o}\Gamma_f^{\rm o} = 2\sqrt{2}\beta^2(\mathcal{F}_0 r_0\varepsilon_\perp - \mathcal{F}_\perp r_\perp\varepsilon_0), \quad (99)$$

$$\pi A_9^{\rm o}\Gamma_f^{\rm o} = 3\beta^2(\mathcal{F}_\perp r_\perp\varepsilon_\parallel - \mathcal{F}_\parallel r_\parallel\varepsilon_\perp). \quad (100)$$

In analogy with the previous solutions of P_2 and P_3 in Eqs. (70) and (74) using the three sets (Set-I, II, III) we can solve for P_2 and P_3 once again in terms of P_1 and "true observables" as

$$\mathsf{P}_2 = \frac{2\mathsf{P}_1 A_{\rm FB}^{\rm o}\left(F_\perp^{\rm o} - \frac{\mathcal{T}_\perp}{\Gamma_f^{\rm o}}\right)}{\sqrt{2}A_5^{\rm o}(2(F_\perp^{\rm o} - \frac{\mathcal{T}_\perp}{\Gamma_f^{\rm o}}) + Z_1^{\rm o}\mathsf{P}_1) - Z_2^{\rm o}\mathsf{P}_1 A_{\rm FB}^{\rm o}}, \quad (101)$$

$$\mathsf{P}_3 = \frac{2\mathsf{P}_1 A_{\rm FB}^{\rm o}\left(F_\perp^{\rm o} - \frac{\mathcal{T}_\perp}{\Gamma_f^{\rm o}}\right)}{(A_{\rm FB}^{\rm o} + \sqrt{2}A_5^{\rm o})\left(2\left(F_\perp^{\rm o} - \frac{\mathcal{T}_\perp}{\Gamma_f^{\rm o}}\right) + Z_1^{\rm o}\mathsf{P}_1\right) - Z_3^{\rm o}\mathsf{P}_1 A_{\rm FB}^{\rm o}}, \quad (102)$$

where positive sign ambiguity is chosen for P_2 and P_3 solutions because of the same reason discussed in the massless case. The definitions of $Z_1^{\rm o}$, $Z_2^{\rm o}$ and $Z_3^{\rm o}$ are given by

$$Z_1^{\rm o} = \sqrt{4\left(F_\parallel^{\rm o} - \frac{\mathcal{T}_\parallel}{\Gamma_f^{\rm o}}\right)\left(F_\perp^{\rm o} - \frac{\mathcal{T}_\perp}{\Gamma_f^{\rm o}}\right) - \frac{16}{9}\beta^2 {A_{\rm FB}^{\rm o}}^2}, \quad (103)$$

$$Z_2^{\rm o} = \sqrt{4\left(F_L^{\rm o} - \frac{\mathcal{T}_0}{\Gamma_f^{\rm o}}\right)\left(F_\perp^{\rm o} - \frac{\mathcal{T}_\perp}{\Gamma_f^{\rm o}}\right) - \frac{32}{9}\beta^2 A_5^{\rm o 2}}, \quad (104)$$

$$Z_3^{\rm o} = \sqrt{4\left(\left(F_L^{\rm o} - \frac{\mathcal{T}_0}{\Gamma_f^{\rm o}}\right) + \left(F_\parallel^{\rm o} - \frac{\mathcal{T}_\parallel}{\Gamma_f^{\rm o}}\right) + \sqrt{2}\pi A_4^{\rm o} - \frac{4\beta^2\varepsilon_0\varepsilon_\parallel}{\Gamma_f^{\rm o}}\right)\left(F_\perp^{\rm o} - \frac{\mathcal{T}_\perp}{\Gamma_f^{\rm o}}\right) - \frac{16}{9}\beta^2(A_{\rm FB}^{\rm o} + \sqrt{2}A_5^{\rm o})^2}. \quad (105)$$

To simplify notation we have defined

$$\mathcal{T}_\lambda = \mathbb{T}_1 + 2\beta^2\varepsilon_\lambda^2; \qquad \lambda \in \{0, \perp, \parallel\}. \quad (106)$$

Substituting Eqs. (101) and (102) in Eq. (53) we can get the condition valid over whole q^2 range as

$$Z_3^{\rm o} = Z_1^{\rm o} + Z_2^{\rm o}. \quad (107)$$

The ε_λ's can be solved as was done in the previous section using Eqs. (98)–(100) to give

$$\varepsilon_\perp = \frac{\sqrt{2}\pi\Gamma_f^{\rm o}}{\beta^2(r_0 - r_\parallel)\mathcal{F}_\perp}\left[\frac{A_9^{\rm o}\mathsf{P}_1}{3\sqrt{2}} + \frac{A_8^{\rm o}\mathsf{P}_2}{4} - \frac{A_7^{\rm o}\beta\mathsf{P}_1\mathsf{P}_2 r_\perp}{3\pi\hat{C}_{10}}\right], \quad (108)$$

$$\varepsilon_\parallel = \frac{\sqrt{2}\pi\Gamma_f^{\rm o}}{\beta^2(r_0 - r_\parallel)\mathcal{F}_\perp}\left[\frac{A_9^{\rm o} r_0}{3\sqrt{2}r_\perp} + \frac{A_8^{\rm o}\mathsf{P}_2 r_\parallel}{4\mathsf{P}_1 r_\perp} - \frac{A_7^{\rm o}\beta\mathsf{P}_2 r_\parallel}{3\pi\hat{C}_{10}}\right], \quad (109)$$

$$\varepsilon_0 = \frac{\sqrt{2}\pi\Gamma_f^{\rm o}}{\beta^2(r_0 - r_\parallel)\mathcal{F}_\perp}\left[\frac{A_9^{\rm o}\mathsf{P}_1 r_0}{3\sqrt{2}\mathsf{P}_2 r_\perp} + \frac{A_8^{\rm o} r_\parallel}{4r_\perp} - \frac{A_7^{\rm o}\beta\mathsf{P}_1 r_0}{3\pi\hat{C}_{10}}\right]. \quad (110)$$

From Eqs. (A10)–(A12) it can be easily seen that the $(\varepsilon_\lambda/\Gamma_f^{\rm o\frac{1}{2}})$'s are free from the form factor $\mathcal{F}_\perp$ and $\Gamma_f^{\rm o}$ *and are completely expressed in terms of observables and the form-factor ratio* P_1. Accurate solutions of $(\varepsilon_\lambda/\Gamma_f^{\rm o\frac{1}{2}})$'s can be found with a few iterations as described in the previous massless case.

Solving for A_4^o from Eq. (107) the relation among the observables including lepton masses turns out

$$A_4^o = \frac{2\sqrt{2}\beta^2 \varepsilon_\parallel \varepsilon_0}{\pi \Gamma_f^o} + \frac{8\beta^2 A_5^o A_{FB}^o}{9\pi\left(F_\perp^o - \frac{\mathcal{T}_\perp}{\Gamma_f^o}\right)} + \sqrt{2}\frac{\sqrt{\left(F_L^o - \frac{\mathcal{T}_0}{\Gamma_f^o}\right)\left(F_\perp^o - \frac{\mathcal{T}_\perp}{\Gamma_f^o}\right) - \frac{8}{9}\beta^2 A_5^{o2}}\sqrt{\left(F_\parallel^o - \frac{\mathcal{T}_\parallel}{\Gamma_f^o}\right)\left(F_\perp^o - \frac{\mathcal{T}_\perp}{\Gamma_f^o}\right) - \frac{4}{9}\beta^2 A_{FB}^{o2}}}{\pi\left(F_\perp^o - \frac{\mathcal{T}_\perp}{\Gamma_f^o}\right)}. \quad (111)$$

In analogy to the massless case, each of Z_1^o, Z_2^o and Z_3^o are also real. A real Z_1^o implies that

$$F_\parallel^o F_\perp^o - \frac{4}{9}A_{FB}^{o2} \geq F_\parallel^o F_\perp^o\left(\frac{\mathcal{T}_\parallel}{\Gamma_f^o F_\parallel^o} + \frac{\mathcal{T}_\perp}{\Gamma_f^o F_\perp^o} - \frac{\mathcal{T}_\parallel \mathcal{T}_\perp}{\Gamma_f^{o2} F_\parallel^o F_\perp^o}\right) - \frac{16m^2 A_{FB}^{o2}}{9q^2}. \quad (112)$$

Since, $0 \leq \frac{\mathcal{T}_\lambda}{\Gamma_f F_\lambda^o} \leq 1$ as can be seen from Eqs. (92)–(94), we can obtain a bound on the lhs of Eq. (112). The bounds arising from real Z_1^o, Z_2^o and Z_3^o are

$$F_\parallel^o F_\perp^o - \frac{4}{9}A_{FB}^{o2} \geq -\frac{16m^2 A_{FB}^{o2}}{9q^2}, \quad (113a)$$

$$F_L^o F_\perp^o - \frac{8}{9}A_5^{o2} \geq -\frac{32m^2 A_5^{o2}}{9q^2}, \quad (113b)$$

$$(F_L^o + F_\parallel^o + \sqrt{2}\pi A_4^o)F_\perp^o - \frac{4}{9}(A_{FB}^o + \sqrt{2}A_5^o)^2 \geq -\frac{16m^2(A_{FB}^o + \sqrt{2}A_5^o)^2}{9q^2} \quad (113c)$$

respectively. Clearly the lhs of the above inequalities can, in the worst case, be a small negative number. Comparing this with the massless case we note that while the effect of the imaginary contributions is to restrict the parameter space further the effect of mass dependent terms is to oppose this restriction. The mass term should have the maximum effect at q^2 close to $4m^2$, but as we will see in the next section (Sec. VI) in the limit $q^2 \to 4m^2$ all the asymmetries approach zero. The contribution from the mass term should hence be insignificant, indicating that in practice the allowed parameter space of observables is not noticeably altered. This conclusion is borne out to be true in numerical estimates as we will see in Sec. VII. We conclude, therefore, that the most conservative allowed parameter space remains unaltered even if the small lepton mass term is dropped compared to q^2 and the imaginary contributions to the amplitudes are completely ignored.

The zero crossings of angular asymmetries A_{FB}^o, A_5^o and $A_{FB}^o + \sqrt{2}A_5^o$ provide interesting limits where the relation in Eq. (111) simplifies to three independent relations with each of them providing an interesting test for NP. At the zero crossing of A_{FB}^o, A_5^o and $A_{FB}^o + \sqrt{2}A_5^o$, Eq. (111) reduces to

$$\frac{8A_5^{o2}}{9\left(F_L^o - \frac{\mathcal{T}_0}{\Gamma_f^o}\right)\left(F_\perp^o - \frac{\mathcal{T}_\perp}{\Gamma_f^o}\right)} + \frac{\pi^2\left(A_4^o - \frac{2\sqrt{2}\beta^2\varepsilon_\parallel\varepsilon_0}{\pi\Gamma_f^o}\right)^2}{2\left(F_L^o - \frac{\mathcal{T}_0}{\Gamma_f^o}\right)\left(F_\parallel^o - \frac{\mathcal{T}_\parallel}{\Gamma_f^o}\right)} = 1 \quad (114a)$$

$$\frac{4A_{FB}^{o2}}{9\left(F_\parallel^o - \frac{\mathcal{T}_\parallel}{\Gamma_f^o}\right)\left(F_\perp^o - \frac{\mathcal{T}_\perp}{\Gamma_f^o}\right)} + \frac{\pi^2\left(A_4^o - \frac{2\sqrt{2}\beta^2\varepsilon_\parallel\varepsilon_0}{\pi\Gamma_f^o}\right)^2}{2\left(F_L^o - \frac{\mathcal{T}_0}{\Gamma_f^o}\right)\left(F_\parallel^o - \frac{\mathcal{T}_\parallel}{\Gamma_f^o}\right)} = 1 \quad (114b)$$

$$\frac{2(A_{FB}^{o2} + 2A_5^{o2})\left(\left(F_L^o - \frac{\mathcal{T}_0}{\Gamma_f^o}\right) + \left(F_\parallel^o - \frac{\mathcal{T}_\parallel}{\Gamma_f^o}\right) + \sqrt{2}\pi A_4^o - \frac{4\beta^2\varepsilon_0\varepsilon_\parallel}{\Gamma_f^o}\right)}{9\left(F_\parallel^o - \frac{\mathcal{T}_\parallel}{\Gamma_f^o}\right)\left(F_L^o - \frac{\mathcal{T}_0}{\Gamma_f^o}\right)\left(F_\perp^o - \frac{\mathcal{T}_\perp}{\Gamma_f^o}\right)} + \frac{\pi^2\left(A_4^o - \frac{2\sqrt{2}\beta^2\varepsilon_\parallel\varepsilon_0}{\pi\Gamma_f^o}\right)^2}{2\left(F_L^o - \frac{\mathcal{T}_0}{\Gamma_f^o}\right)\left(F_\parallel^o - \frac{\mathcal{T}_\parallel}{\Gamma_f^o}\right)} = 1 \quad (114c)$$

respectively. In the limit where both the mass effect and the imaginary contributions to the Wilson coefficients $\hat{C}_7$ and $\hat{C}_9$ can be ignored these relations simplify to depend only on observables

$$\frac{8A_5^2}{9F_L F_\perp} + \frac{\pi^2 A_4^2}{2F_L F_\parallel} = 1 \quad \text{if } A_{FB} = 0$$

$$\frac{4A_{FB}^2}{9F_\parallel F_\perp} + \frac{\pi^2 A_4^2}{2F_L F_\parallel} = 1 \quad \text{if } A_5 = 0$$

$$\frac{2(A_{FB}^2 + 2A_5^2)(F_L + F_\parallel + \sqrt{2}\pi A_4)}{9F_\parallel F_L F_\perp} + \frac{\pi^2 A_4^2}{2F_L F_\parallel} = 1 \quad \text{if } A_{FB} + \sqrt{2}A_5 = 0. \quad (115)$$

The zero crossings of these observables are also interesting as the form-factor ratios P_1, P_2 and P_3 can be related to the helicity fractions at those q^2 points. Equation (97) implies that when $A_{FB}^o = 0$, $r_\parallel + r_\perp$ must be zero. Then, the expression for $r_\parallel + r_\perp$ [see Eq. (A10) for the massive case in Appendix A] gives

$$r_\parallel + r_\perp|_{A_{\rm FB}^{\rm o}=0} = \pm\frac{\sqrt{\Gamma_f^{\rm o}}}{\sqrt{2}\mathcal{F}_\perp}\left(\sqrt{F_\perp^{\rm o}-\frac{\mathcal{T}_\perp}{\Gamma_f^{\rm o}}}+\mathsf{P}_1\sqrt{F_\parallel^{\rm o}-\frac{\mathcal{T}_\parallel}{\Gamma_f^{\rm o}}}\right)=0$$

$$\Rightarrow \mathsf{P}_1|_{A_{\rm FB}^{\rm o}=0} = -\frac{\sqrt{F_\perp^{\rm o}-\frac{\mathcal{T}_\perp}{\Gamma_f^{\rm o}}}}{\sqrt{F_\parallel^{\rm o}-\frac{\mathcal{T}_\parallel}{\Gamma_f^{\rm o}}}} \tag{116}$$

P_1 can be iteratively solved from the above equation. We note that in order one has real positive form factors by definition [Eq. (51)] P_1 is always negative. The zero crossing of $A_{\rm FB}^{\rm o}$ is observed at $q^2 = 4.9^{+1.1}_{-1.3}$ GeV^2 [5] which is in the large recoil region where it is believed that reliable calculations can be done in HQET. Hence, we can check the predictability of HQET in large recoil region, when enough data for all observables are available at this q^2 point.

Equations (101) and (102) can now be used to obtain P_2 and P_3 at the zero crossings $A_5^{\rm o}=0$ and $A_{\rm FB}^{\rm o}+\sqrt{2}A_5^{\rm o}=0$ respectively,

$$\mathsf{P}_2|_{A_5^{\rm o}=0} = -\frac{\sqrt{F_\perp^{\rm o}-\frac{\mathcal{T}_\perp}{\Gamma_f^{\rm o}}}}{\sqrt{F_L^{\rm o}-\frac{\mathcal{T}_0}{\Gamma_f^{\rm o}}}}, \tag{117}$$

$$\mathsf{P}_3\Big|_{A_{\rm FB}^{\rm o}+\sqrt{2}A_5^{\rm o}=0} = -\frac{\sqrt{F_\perp^{\rm o}-\frac{\mathcal{T}_\perp}{\Gamma_f^{\rm o}}}}{\sqrt{\left(\left(F_L^{\rm o}-\frac{\mathcal{T}_0}{\Gamma_f^{\rm o}}\right)+\left(F_\parallel^{\rm o}-\frac{\mathcal{T}_\parallel}{\Gamma_f^{\rm o}}\right)+\sqrt{2}\pi A_4^{\rm o}-\frac{4\beta^2\varepsilon_0\varepsilon_\parallel}{\Gamma_f^{\rm o}}\right)}}. \tag{118}$$

The relation derived in Eq. (111) incorporates all the possible effects within SM. It includes a finite lepton mass, electromagnetic correction to hadronic operators at all orders and all factorizable and nonfactorizable contributions including resonances to the decay. It can be seen from the Eq. (106) the term $\mathcal{T}_\lambda/\Gamma_f^{\rm o}$ contains $\mathbb{T}_1/\Gamma_f^{\rm o}$ which is expressed in Eq. (88) in terms of the asymmetries A_{10} and A_{11} which can be measured experimentally and the other term $(\varepsilon_\lambda/\Gamma_f^{\rm o\frac{1}{2}})$ depends only on the observables and one form-factor ratio P_1. Thus, the relation in Eq. (111) is complete and exact in the sense that it involves all the eleven observables and only one hadronic input which can be reliably estimated using HQET.

VI. OBSERVABLES AT KINEMATIC EXTREME POINTS

In this section we will briefly discuss the limiting value of the observables at the two kinematic extremities of q^2, the dilepton invariant mass squared. The minimum q^2 value, $q^2 = q^2_{\rm min} = 4m^2$ and the endpoint $q^2 = q^2_{\rm max} = (m_B - m_{K^*})^2$. The values of the observables we obtain below can be experimentally verified and any exception must imply NP.

(i) *Case-I:* $q^2 = 4m^2$

It is easy to see that at $q^2_{\rm min}$ the two leptons carry equal momentum and recoil against the K^*. In the dilepton rest frame the two leptons carry zero momentum. Hence, angles θ_ℓ and ϕ cannot be defined. The angular distribution in Eq. (13) thus implies that all asymmetries i.e. A_4, A_5, $A_{\rm FB}$, A_7, A_8 and A_9 must vanish in this limit. This implies that there is no preferred direction, leading to the conclusion that all helicities are equally probable.

Using the expressions of the observables derived in the previous section [Eqs. (85a) and (85b)] we can write

$$F_L^{\rm o} = \frac{1}{\Gamma_f^{\rm o}}\left(\beta^2\Gamma_f F_L + \frac{1}{3}(\Gamma_f^{\rm o}-\beta^2\Gamma_f)\right) \underset{\beta\to 0}{=} \frac{1}{3}. \tag{119}$$

This limiting value holds for the other two helicity fractions as well. Hence, at the kinematic starting point we can write

$$F_{\lambda\ q^2\to 4m^2}^{\rm o} = \frac{1}{3}, \qquad \lambda \in \{L,\perp,\parallel\}. \tag{120}$$

We conclude that each observed helicity fraction should be $1/3$ at $q^2_{\rm min}$, which can be easily verified experimentally. The asymmetries defined in Eqs. (89) and (90) also vanish at $q^2 = q^2_{\rm min}$ implying $(\mathbb{T}_1/\Gamma_f^{\rm o}) \to \frac{1}{3}$ [from Eq. (88)]. Thus the observable $A_4^{\rm o}$ from Eq. (111) at $q^2 = q^2_{\rm min}$ is given by

$$A_{4\ \beta\to 0}^{\rm o} = \frac{\sqrt{2}}{\pi}\sqrt{F_L^{\rm o}-\frac{\mathbb{T}_1}{\Gamma_f^{\rm o}}}\sqrt{F_\parallel^{\rm o}-\frac{\mathbb{T}_1}{\Gamma_f^{\rm o}}}\ \underset{\frac{\mathbb{T}_1}{\Gamma_f^{\rm o}}\to\frac{1}{3}}{\underset{F_\lambda^{\rm o}\to\frac{1}{3}}{=}}\ 0 \tag{121}$$

as it was expected above.

(i) *Case-II:* $q^2 = (m_B - m_{K^*})^2$

In this kinematic limit the K^* is at rest and the two leptons go back to back in the B meson rest frame. Therefore, we

can always choose the angle ϕ to be zero. The entire decay takes place in one plane, resulting in vanishing $F_\perp$. Also, the left and right chirality of the leptons contribute equally. These together results in only the angular asymmetry A_4 being finite with all other asymmetries vanishing. The relations among the various angular coefficients at this kinematical endpoint are derived in Ref. [28] where it is explicitly shown that

$$F_L(q^2_{\rm max}) = \frac{1}{3}, \qquad A_{\rm FB}(q^2_{\rm max}) = 0. \tag{122}$$

Solving for the other observables from Eq. (3.2) of Ref. [28] we can write

$$F_\perp(q^2_{\rm max}) = 0, \qquad F_\parallel(q^2_{\rm max}) = \frac{2}{3}, \tag{123}$$

$$A_4(q^2_{\rm max}) = \frac{2}{3\pi}, \qquad A_{5,7,8,9}(q^2_{\rm max}) = 0. \tag{124}$$

These limiting values of the observables imply that $\varepsilon_\lambda \to 0$ at the extremum $q^2 = q^2_{\rm max}$ as can be seen from Eqs. (108)–(110). The lepton mass can be safely ignored at $q^2_{\rm max}$ as it would have almost no effect at this end point hence, we have dropped the "o" index from all the observables for this discussion only. Thus, in the limit $\varepsilon_\lambda \to 0$, we find that Eq. (111) reduces to Eq. (80). Hence, the observable A_4 at $q^2 = q^2_{\rm max}$ turns out to be

$$A_4 = \frac{8A_5A_{\rm FB}}{9\pi F_\perp} + \sqrt{2}\frac{\sqrt{F_LF_\perp - \frac{8}{9}A_5^2}\sqrt{F_\parallel F_\perp - \frac{4}{9}A_{\rm FB}^2}}{\pi F_\perp} = \underset{A_5\to 0}{\overset{A_{\rm FB}\to 0}{=}} \frac{\sqrt{2}\sqrt{F_LF_\parallel}}{\pi} \underset{F_\parallel\to\frac{2}{3}}{\overset{F_L\to\frac{1}{3}}{=}} \frac{2}{3\pi}$$

which exactly matches with the limit predicted in Eq. (124).

VII. NEW PHYSICS ANALYSIS

In this section, we demonstrate the possibility of how new physics could be tested using the relations derived in this paper. The basis of our analysis is the relation, which involves all the nine observables F_L, $F_\parallel$, $F_\perp$, $A_{\rm FB}$, A_4, A_5, A_7, A_8, A_9 and a single form-factor ratio P_1 derived in Eq. (79). Since the helicity fractions are related by $F_L + F_\parallel + F_\perp = 1$, we eliminate $F_\parallel$. All the observables have been measured by LHC*b* Collaboration using 1 fb^{-1} data. However, currently the observables A_7, A_8 and A_9 are measured to be consistent with zero. Equations (108)–(110) therefore imply that ε_λ are all consistent with zero. In Sec. V we have shown that the most conservative allowed parameter space remains unaltered even if the small lepton mass term is dropped compared to q^2 and the imaginary contributions to the amplitudes are completely ignored. Since the inclusion of ε_λ reduces the parameter space of observables, in order to check the consistency of measured observables we take a conservative approach and set all the ε_λ's to be equal to zero for the numerical analysis. Thus, the relation among the observables reduces to Eq. (80) which is in terms of six observables F_L, $F_\parallel$, $F_\perp$, $A_{\rm FB}$, A_4, A_5 and is completely free from any form-factor dependence. If A_7, A_8 and A_9 are measured to be nonzero in future experiments with reduced uncertainties, ε_λ can be solved iteratively using Eqs. (108)–(110) and an exact numerical analysis can always be done. We, emphasize that a nonzero ε_λ would only restrict the allowed parameter space depicted in Figs. 1, 2 and 3 further as was already pointed out in Sec. V. Later in this section we will, nevertheless, solve for ε_λ in terms of A_7, A_8 and A_9 since the predicted value $A_4^{\rm pred}$ depends on the values of ε_λ.

We use the SM relation derived in Eq. (80), for $\varepsilon_\lambda = 0$ and $4m^2/q^2 \to 0$ instead of Eq. (111), to check for consistency between measurements of all the observables. As noted above a finite value for ε_λ would provide a stronger constraint and since ε_λ's are consistent with zero, Eq. (80) provides a more conservative test. In order to perform the test we define a χ^2 function

$$\chi^2 = \frac{1}{4}\left[\left(\frac{A_4^{\rm exp} - A_4^{\rm pred}}{\Delta A_4^{\rm exp}}\right)^2 + \left(\frac{F_L^{\rm exp} - F_L}{\Delta F_L^{\rm exp}}\right)^2 + \left(\frac{F_\perp^{\rm exp} - F_\perp}{\Delta F_\perp^{\rm exp}}\right)^2 + \left(\frac{A_{\rm FB}^{\rm exp} - A_{\rm FB}}{\Delta A_{\rm FB}^{\rm exp}}\right)^2 + \left(\frac{A_5^{\rm exp} - A_5}{\Delta A_5^{\rm exp}}\right)^2\right], \tag{125}$$

where $A_4^{\rm exp}, F_L^{\rm exp}, F_\perp^{\rm exp}, A_{\rm FB}^{\rm exp}, A_5^{\rm exp}$ indicate experimental central values of the observables and $\Delta A_4^{\rm exp}, \Delta F_L^{\rm exp}, \Delta F_\perp^{\rm exp}, \Delta A_{\rm FB}^{\rm exp}, \Delta A_5^{\rm exp}$ are the experimental uncertainties. The statistical and systematic uncertainties are added in quadrature for all the numerical analysis presented. We used Mathematica [29] to do all the numerical calculations presented in this paper. The χ^2 function in Eq. (125) is minimized in the 4-dimensional parameter space of the observables by varying each of them simultaneously within the allowed region i.e. $0 \le F_L \le 1$, $0 \le F_\perp \le 1$, $-1 \le A_{\rm FB} \le 1$, $-1 \le A_5 \le 1$, while $A_4^{\rm pred}$ is taken to be the theoretically calculated value for A_4 using Eq. (80). The minimized χ^2 function is projected in different sets of planes of the observables, $(F_L, F_\perp)$, $(A_{\rm FB}, F_L)$, $(A_{\rm FB}, A_5)$ (A_5, F_L), $(A_5, F_\perp)$ and $(A_{\rm FB}, F_\perp)$ for the contour plots. In Fig. 1 we show the allowed domain of $F_L - F_\perp$ values for all the six q^2 bins corresponding to the q^2 values in the range (0.1–2) GeV^2, (2–4.34) GeV^2, (4.34–8.68) GeV^2, (10.09–12.86) GeV^2, (14.0–16.0) GeV^2 and (16.0–19.0) GeV^2. The pink, yellow and blue correspond to 1σ, 2σ and 3σ confidence level

regions. The black squares correspond to the experimentally measured central value and the green points correspond to best fit values obtained by minimizing χ^2 using Eq. (125). As can be seen form Fig. 1 the bounds derived in this paper, involving only observables, have resulted in very significantly constraining the allowed parameters range of observables.

If it were true that there are no significant nonfactorizable contributions to the decay mode, rendering $\tilde{C}_9^\lambda$ independent of the helicity index "λ," we can solve for $\tilde{C}_9$ as was shown in Ref. [2]. The ratio of $\tilde{C}_9/\hat{C}_{10}$ so obtained could be inverted to solve for $A_{\rm FB}$ resulting in the constraint between F_L and $F_\perp$ given in Eq. (55) of Ref. [2]. The narrow constraint region between the two solid black lines depicted in $F_L - F_\perp$ plane in Fig. 1 is derived assuming real transversity amplitudes, form factors are calculated at leading order in $\Lambda_{\rm QCD}/m_b$ using HQET and the estimate that $\tilde{C}_9/\hat{C}_{10} = -1$ is used. We emphasize that except for the two solid black lines for each of the q^2 bins all other information in Fig. 1 is completely free from any theoretical assumption. As can be seen from Fig. 1 the best fit values as well as the experimentally measured central values are largely not inside the narrow constraint region within two solid black lines. This indicates that there could exist any or all of the possibilities: imaginary contributions to the transversity amplitudes or sizable nonfactorizable contributions or higher order corrections in HQET could also be relevant.

The allowed range for observables $A_{\rm FB} - F_L$ is depicted in Fig. 2 for all the six bins. The color code and markers follow the same convention used in Fig. 1. The constraint of the allowed triangular region between two solid black line comes from Eq. (53) of Ref. [2]. Once again the constraint region within the solid black triangular depicted in $A_{\rm FB} - F_L$ plane is derived assuming real transversity amplitudes, form factors calculated at leading order in $\Lambda_{\rm QCD}/m_b$ using HQET and the estimate that $\tilde{C}_9/\hat{C}_{10} = -1$. However, note that the constraints depicted by the contour plots are completely free from any theoretical assumptions. The allowed region in the other four planes of observables i.e. $A_{\rm FB} - A_5$, $A_5 - F_L$, $A_5 - F_\perp$ and $A_{\rm FB} - F_\perp$ are shown in Fig. 3. We emphasize once again that the plots are free from any

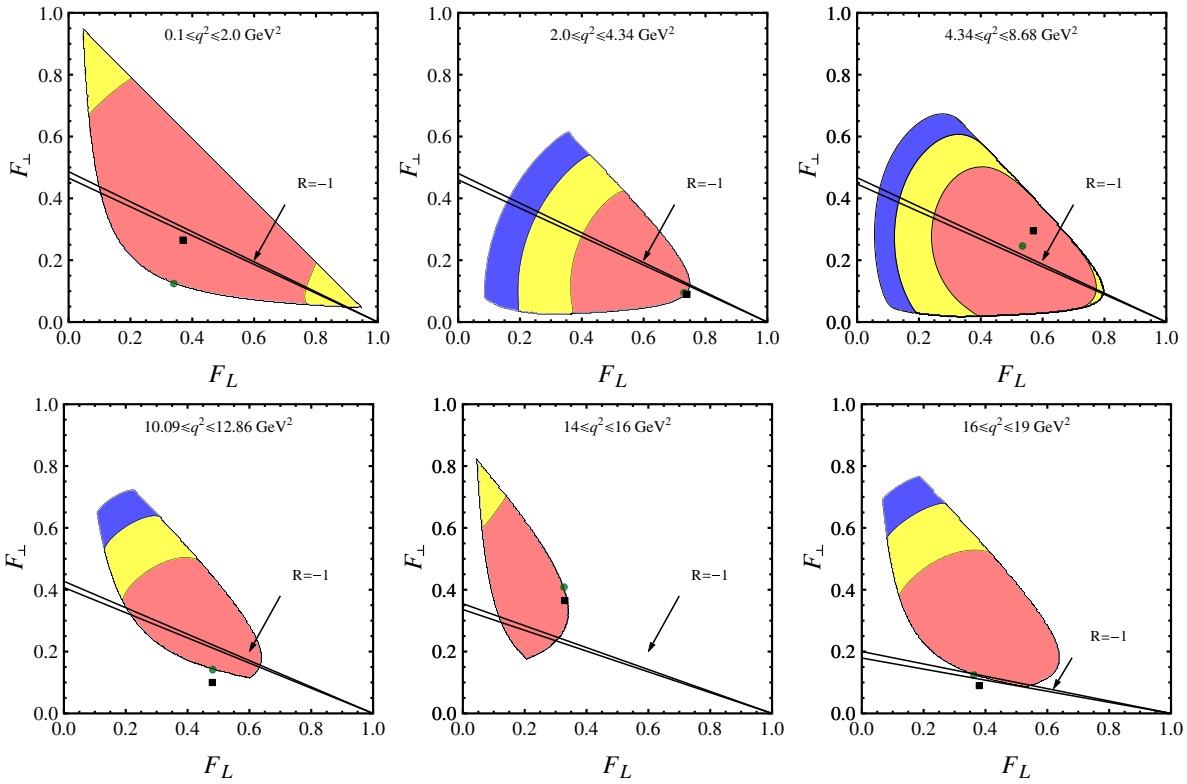

FIG. 1 (color online). The χ^2 projection onto the plane of observables F_L and $F_\perp$. The experimental values of all the observables are taken from 1 fb^{-1} LHCb measurements Ref. [5]. The green dots corresponds to best fit value from χ^2 minimization and the black squares corresponds to the measured central value. The pink (dark), yellow (light) and blue (darkest) correspond to the 1σ, 2σ and 3σ confidence level regions respectively. If the amplitudes are real, nonfactorizable contributions vanish and the form factors were reliably evaluated at leading order in HQET, then using SM estimated values of Wilson coefficients we find $F_L - F_\perp$ are constrained to lie in the narrow region between the two solid black lines. See text for details.

theoretical uncertainty. In most of the contour plots depicted in Figs. 1, 2 and 3 the best fit points (green point) lie at the edge of the boundaries except for the third bin. The experimental measured central values (black squares) are mostly overlapping with the best fit points except for fourth and sixth bin. In the fourth bin the black squares stay outside the physically allowed region. In third bin both the best fit and experimental measurement are very consistent with the allowed region and sit almost at the center of it. It is interesting to note that the best fits are always in the 1σ region perhaps validating the LHCb data set.

In Fig. 4 the measured Gaussian A_4 distribution is compared with the distribution of $A_4^{\rm pred}$ computed using Eq. (80). In evaluating the right-hand side of Eq. (80) we have used a Gaussian distribution of the observables F_L, $F_\perp$, A_5 and $A_{\rm FB}$ with experimental central value as the mean and errors as the standard deviation from Ref. [5]. The plots correspond to a simulated theory sample of 144, 76, 281, 169, 114 and 124 events corresponding to first through sixth q^2 bins. These may be compared with 140, 73, 271, 168, 115 and 116 events obtained for the respective bins by LHCb using 1 fb^{-1} data [5]. We have randomly chosen the number of events to be statistically consistent with the LHCb observation in each bin for this decay mode. As should be expected fewer events survive the constraint of Eq. (80) when the best fit points are at the edge of the permissible contour regions in Figs. 1, 2 and 3. The simulated A_4 values corresponding to the LHCb measurement for all six bins are shown in red (dark) histogram and the yellow (light) histogram corresponds to the values of $A_4^{\rm pred}$ computed using Eq. (80). For a comparison, the probability distribution function (PDF) curves corresponding to 1000 times more events are also shown for theory using brown (light) curve and data using red (dark) curve.

The mean and 1σ regions for the theoretically calculated $A_4^{\rm pred}$ distributions are shown in Fig. 5. We compare the two cases where lepton masses is ignored [Eq. (80)] with the case where lepton mass is finite [Eq. (111)]. The purple (light) bands correspond to the massless case and the gray (dark) band corresponds to the massive case. The error bars in red correspond to the experimentally measured [5] central values and errors in A_4 for the respective q^2 bins. The values of $A_4^{\rm pred}$ obtained from the Eq. (80) seem to visually agree reasonably with the experimental measurements within the error bands in all the bins except for the first and the fifth bin. A large discrepancy in fifth bin can

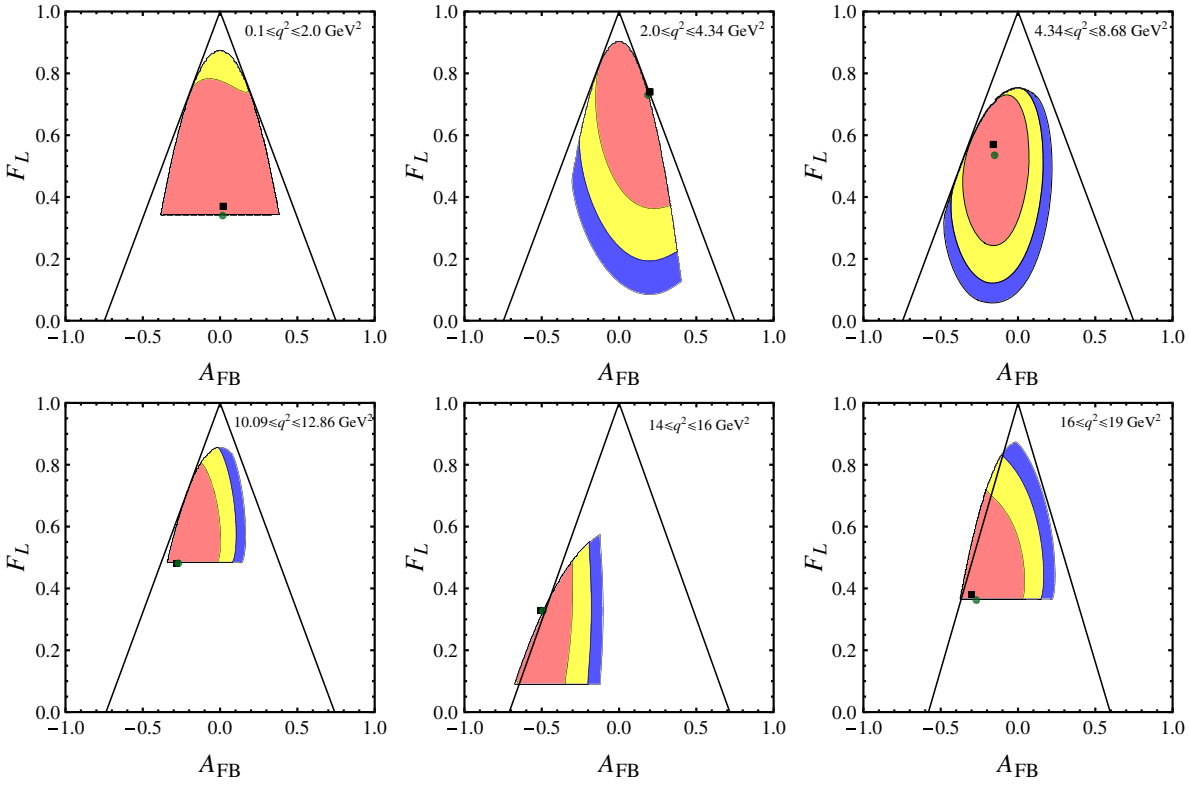

FIG. 2 (color online). The χ^2 projection onto the plane of observables F_L and $A_{\rm FB}$. The experimental values of all the observables are taken from Ref. [5]. The color codes are the same as in Fig. 1. If the amplitudes are real, nonfactorizable contributions vanish and the form factors were reliably evaluated at leading order in HQET then using SM estimated values of Wilson coefficients we find $A_{\rm FB} - F_L$ are constrained to lie in the two solid black triangular region. See text for details.

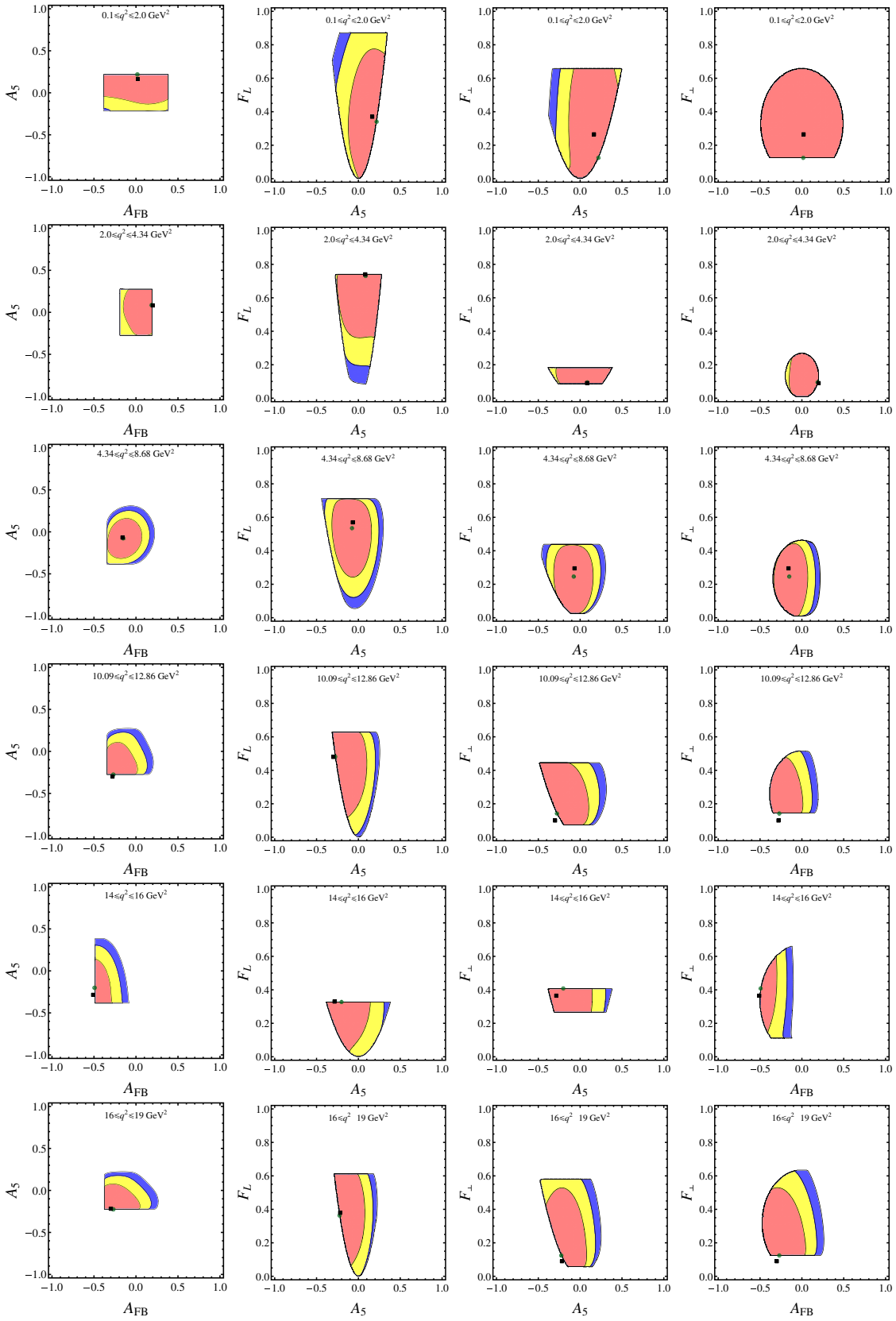

FIG. 3 (color online). The χ^2 projection onto the sets observables $A_5 - A_{\rm FB}$, $A_5 - F_L$, $A_5 - F_\perp$ and $A_{\rm FB} - F_\perp$ for various q^2 bins going vertically from first to the sixth bin. The experimental values of all the observables are taken from Ref. [5]. The color codes are same as in Fig. 1.

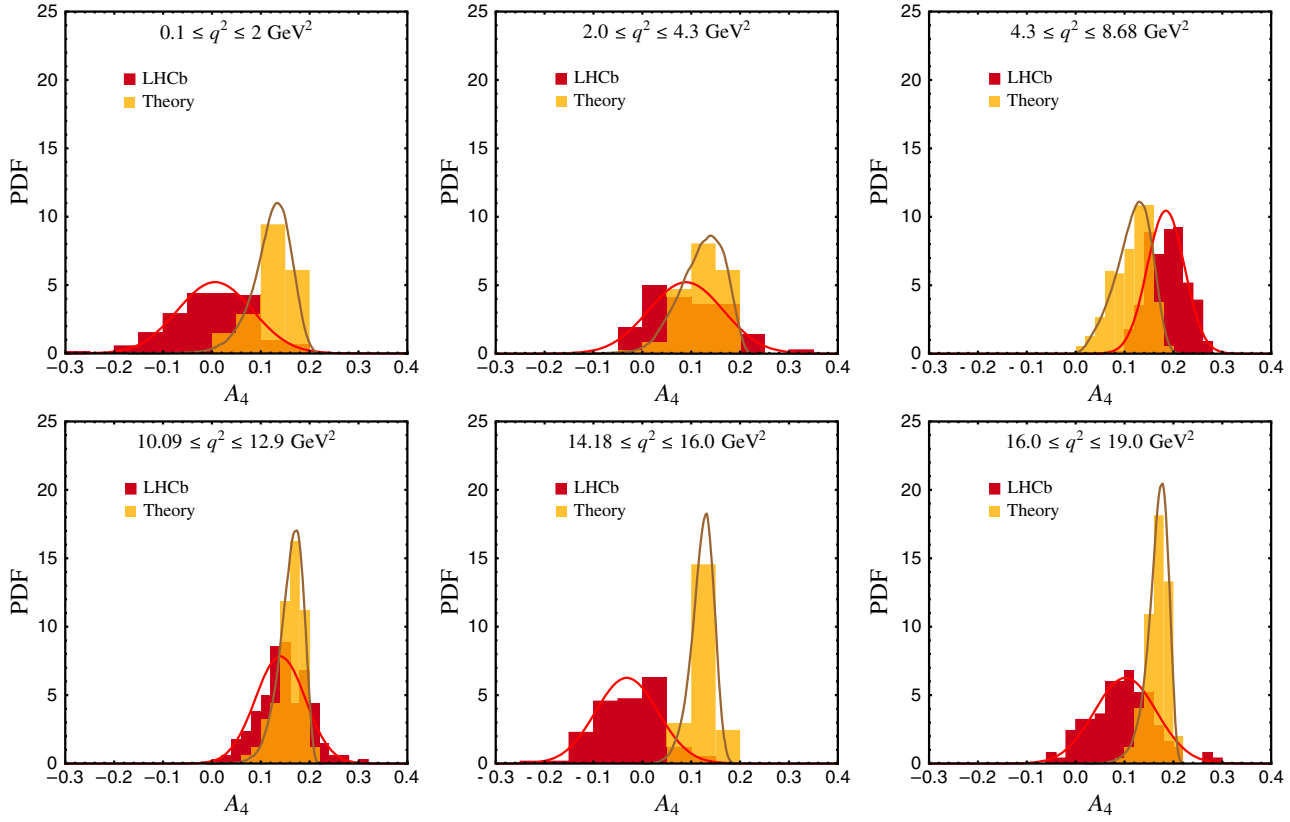

FIG. 4 (color online). A comparison of the measured and the predicted A_4 values for the six q^2 bins assuming that A_7, A_8 and A_9 are all zero. The simulated values of A_4 assuming Gaussian error in the LHCb data are shown in red (dark), whereas the yellow (light) distributions referred to as "Theory" correspond to the values of $A_4^{\rm pred}$ computed using Eq. (80). The plots correspond to a simulated theory (LHCb 1 fb^{-1} data [5]) sample of 144 (140), 76 (73), 281 (271), 169 (168), 114 (115) and 124 (116) events corresponding to first through sixth q^2 bins as depicted in the figure. We have randomly chosen the events to be statistically consistent with the LHCb observation in each bin for this decay mode. For a comparison, the PDF curves corresponding to 1000 times more events are also shown for theory using brown (light) curve and data using red (dark) curve. We compare the two simulated distributions shown in the histograms using the Mathematica routine "DistributionFitTest" [30]. The P-values obtained by comparing the two are found to be less than 10^{-9} for each of the bins, except the second and fourth bins, where the P-values obtained are 2.54×10^{-5} and 6.47×10^{-6} respectively.

also be seen here. There is also a slight tension in first bin, which could be partly due to the lepton mass effect. The corrections due to mass terms can be incorporated if the asymmetries A_{10} and A_{11} are measured in the future. In the absence of such measurements we have used the theoretical estimate of form factors [13] to evaluate the effect of the finite mass contribution. Details are depicted in Fig. 5. The mass contributions only affect the first bin, the other bins are unaffected. As expected the agreement improves for the first bin if the mass contributions are added. While Fig. 5 indicates only a mild disagreement between the measured and predicted values of A_4, the distributions in Fig. 4 carry much more information than the mean and averages. We have compared the two simulated distributions shown in the histograms using the Mathematica routine "DistributionFitTest" [30]. The P-values obtained by comparing the two are found to be less than 10^{-9} for each of the bins, except the second and fourth bins, where the P-values obtained are 2.54×10^{-5} and 6.47×10^{-6} respectively. A small P-value indicates that one should reject the hypothesis that all observables are consistent with the SM relation of Eq. (80).

In order to ascertain that the discrepancy in the A_4 enunciated using the P-values is not due to the imaginary contributions being ignored we have also preformed a simulation of all observables, including A_7 A_8 and A_9. We solved for $\varepsilon_\perp$, $\varepsilon_\parallel$ and ε_0 using Eqs. (108)–(110). These values of $\varepsilon_\perp$, $\varepsilon_\parallel$ and ε_0 depend only on observables and P_1. We assume P_1 values (see Ref. [2]) to be $\mathsf{P}_1 = -0.9395$, -0.9286, -0.9034, -0.8337, -0.7156 and -0.4719 for the first through the sixth bin respectively. We only remark that if A_7, A_8 and A_9 are measured to be small the results are even more insensitive to the choice of the P_1 value. Nevertheless, we also studied the effect of varying P_1

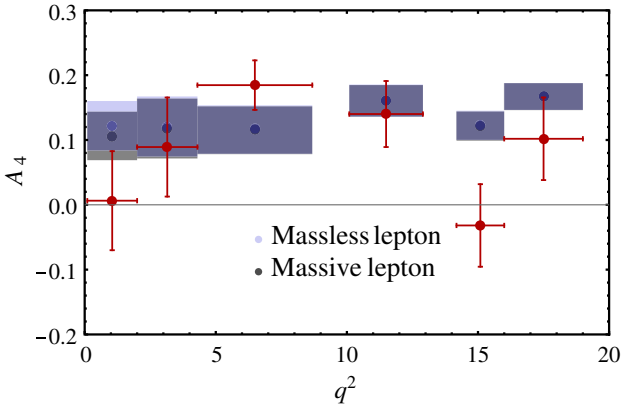

FIG. 5 (color online). The mean values and 1σ regions for theoretically calculated A_4 distributions excluding lepton masses [Eq. (80)] and with massive leptons [Eq. (111)] are shown in purple (light) and gray (dark) bands respectively. The simulated samples consist of 50,000 events to start with, for each bin. The observables A_7, A_8 and A_9 are assumed to be zero. The error bars in red correspond to the experimentally measured [5] central values and errors in A_4 for the respective q^2 bins.

within the range $\mathsf{P}_1 \pm 0.5$, to ascertain our claim. Details will be presented elsewhere. The ε_λ were solved iteratively and it was found that they always converged in just a few iterations. If iteration led to a value of ε_λ larger than the derived constraints permitted, a smaller allowed value was assigned and the iteration continued. In some cases an oscillatory or randomly varying pattern was observed but in these cases the starting values of the observables could not be reproduced, indicating that further constraints imposed by the chosen values of A_7, A_8 and A_9 could not be satisfied. The solutions obtained for $\varepsilon_\lambda/\sqrt{\Gamma_f}$ are shown for each of the six bins in Fig. 6. It can be seen that all the ε_λ's are consistent with zero and even the tails of $\varepsilon_\lambda^2/\Gamma_f$ do not cross 0.2. Having obtained the values of $\varepsilon_\lambda/\sqrt{\Gamma_f}$ we can now use the exact relation in Eq. (111) to estimate $A_4^{\rm pred}$. A comparison between the measured A_4 and the predicted value $A_4^{\rm pred}$ including contributions from A_7, A_8 and A_9 is done in Fig. 7. It must be emphasized that $A_4^{\rm pred}$ obtained using Eq. (111) is exact and takes into account all the contributions in SM. The asymmetries A_{10} and A_{11} [see Eqs. (89) and (90)] have not yet been measured and Fig. 5 indicates that the lepton mass effects are negligible for all but the first bin. We hence set $\mathbb{T}_1 = 0$ in evaluating $A_4^{\rm pred}$. This ensures that our results depend on only one theoretical parameter, the ratio of form factors P_1 and that parameters resulting in unmeasurable tiny effects do not complicate the calculations. As predicted above, an even smaller number of events are now consistent with the constraints derived in the paper. Interestingly, $A_4^{\rm pred}$ now fits better to a Gaussian distribution as indicated by a Kolmogorov-Smirnov test, compared to the previous case where transversity

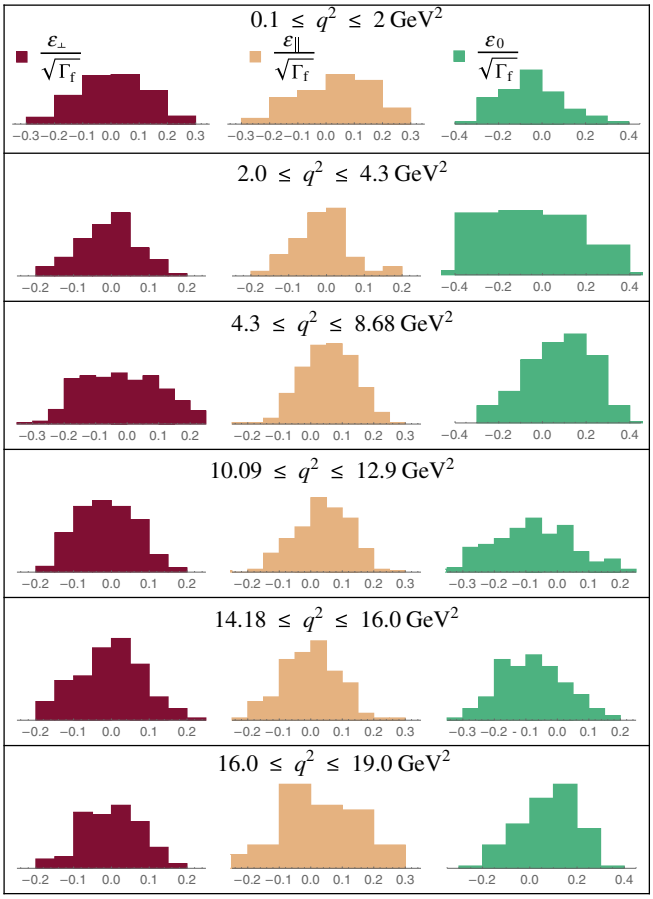

FIG. 6 (color online). The solutions for $\varepsilon_\perp/\sqrt{\Gamma_f}$, $\varepsilon_\parallel/\sqrt{\Gamma_f}$ and $\varepsilon_0/\sqrt{\Gamma_f}$ using distributions with 140, 78, 275, 175, 113 and 113 events for first through sixth q^2 bins. The number of events are chosen to be statistically consistent with the number of events observed by LHCb [5] in each bin for this decay mode. All the ε_λ's are consistent with zero and even at extreme cases $\varepsilon_\lambda^2/\Gamma_f$ values are less than 0.2.

amplitudes were assumed to be real. This is indicative of the fact that the transversity amplitudes are complex. However, the values of $\varepsilon_\lambda/\sqrt{\Gamma_f}$ are not large as indicted in Fig. 6. We have simulated numbers of events consistent statistically with the number of events observed by LHCb in each bin. The plots as depicted in Fig. 7 correspond to a simulated theory (LHCb 1 fb^{-1} data [5]) sample of 140 (140), 78 (73), 275 (271), 175 (168), 113 (115) and 113 (116) events for the first through sixth q^2 bins. The values of $A_4^{\rm pred}$ predicted using Eq. (111) have a larger mean and variance as compared to values obtained using Eq. (80). The P-values still continue to be smaller than 10^{-9} for all the bins, except the second bin where the P-value is 6.78×10^{-3}, indicating that we reject the hypothesis that all observables are consistent with the exact SM relation of Eq. (111).

The PDF curves comparing the measured value of A_4 with both the theoretically predicted values assuming

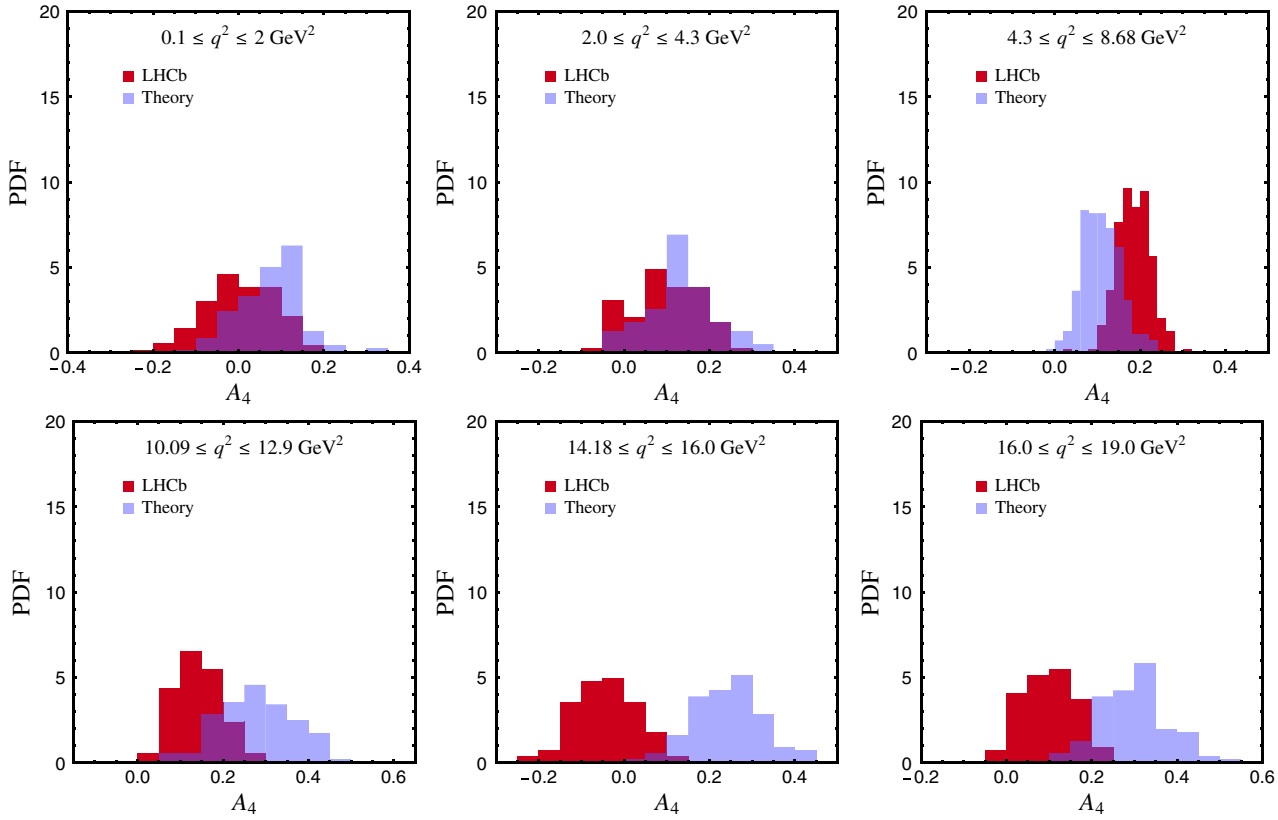

FIG. 7 (color online). A comparison of the measured and predicted A_4 values for the six q^2 bins considering all the measured observables. The simulated values of A_4 assuming Gaussian error in the LHCb data are shown in red (dark), whereas the blue (light) distributions referred to as "Theory" correspond to the values of $A_4^{\rm pred}$ computed using Eq. (111). The plots correspond to a simulated theory (LHCb 1 fb^{-1} data [5]) sample of 140 (140), 78 (73), 275 (271), 175 (168), 113 (115) and 113 (116) events corresponding to first through sixth q^2 bins as depicted in the figure. The number of events are chosen to be consistent statistically with the number of events observed by LHCb in each bin for this decay mode. The values of all other observables used in the two equations are randomly generated using LHCb data assuming Gaussian measurements. We find that the P-values obtained using the Mathematica routine "DistributionFitTest" [30] comparing the two distributions are always less than 10^{-9} for all bins except the second bin where the P-value is 6.78×10^{-3}.

completely real transversity amplitudes ($\varepsilon_\lambda = 0$) and most general complex transversity amplitudes ($\varepsilon_\lambda \neq 0$) are shown in Fig. 8 for fifth bin ($14.0 \leq q^2 \leq 16.0$ GeV^2). We have chosen the fifth bin for this detailed study since the tension between the predicted value and experimentally observed value appears to be the largest as can be seen from Figs. 4, 5 and 7. The PDFs depicted in the figure are generated using 4×10^5 random events resulting in the simulated values of A_4 for each curve. If $\varepsilon_\lambda \neq 0$ only 6708 of the points survived the constraints of Eq. (111). LHCb data assuming Gaussian error is shown in the leftmost red (dark) plot, whereas the central brown (lighter) distribution corresponds to the theoretically calculated A_4 using Eq. (79) and the rightmost blue (light) distribution is for A_4 predicted using Eq. (111). The values of all other observables used in the two equations are randomly generated assuming Gaussian measurements of the LHCb 1 fb^{-1} data.

In this section we have discussed the constraints already imposed by the 1 fb^{-1} LHCb data [5] on the parameter space of observables. We also compare the measured values of A_4 with those predicted using the new relations derived in this paper. We made several observations that indicate possibly sizable nonfactorizable contributions and imaginary contribution and also possible higher order corrections in HQET to the transversity amplitudes. In addition, the P-values comparing the measured A_4 with the predicted value indicates new physics. However, we refrain from drawing even the obvious conclusions given that, results for 3 fb^{-1} data will soon be presented by the LHCb Collaboration. However, we emphasize that the approach developed in this paper could not only conclusively indicate presence of significant nonfactorizable contributions and need for higher order power corrections to form factors but also the presence of NP with larger statistics.

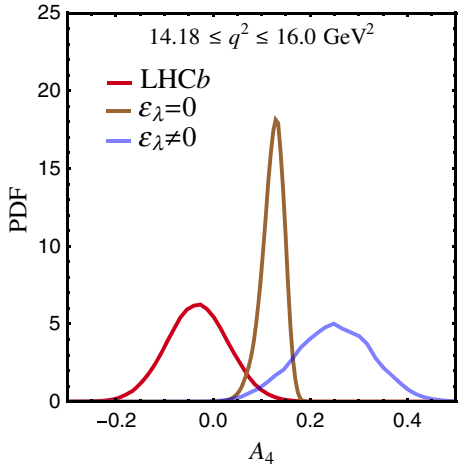

FIG. 8 (color online). A PDF plot comparing the measured fifth bin ($14.0 \le q^2 \le 16.0$ GeV^2) value of A_4 with the two theoretically predicted values. One assuming $\varepsilon_\lambda = 0$ or completely real transversity amplitudes and the other with $\varepsilon_\lambda \neq 0$ or complex transversity amplitudes. The mean and errors for all the observables are assumed to be those measured by LHCb using 1 fb^{-1} data set. All errors are assumed to be Gaussian. The PDFs depicted in the figure are generated using 4×10^5 random events resulting in the simulated values of A_4 for each curve. If $\varepsilon_\lambda \neq 0$ only 6708 of the points survived the constraints. The plot corresponding to LHCb A_4 measurement is shown in left most red (dark) plot, whereas the central brown (lighter) distribution corresponds to the theoretically calculated A_4 using Eq. (79) and the right most blue (light) distribution is for A_4 predicted using Eq. (111).

VIII. CONCLUSIONS

In this paper we have derived a new relation involving all the CP conserving observables that can be measured in the decay $B \to K^* \ell^+ \ell^-$ using an angular study of the final state for the decay. The relation provides a very clean and sensitive way to test SM and search for NP by probing consistency between the measured observables. The relation reduces to the one derived in Ref. [2], when certain reasonable assumptions were made. Since, the relation is intended to be used as probe in search for NP, it is imperative that no avoidable assumptions be made. We have generalized previous results with this objective in mind. The new derivation is parametrically *exact in the SM limit* and incorporates finite lepton and quark masses, complex amplitudes enabling resonance contributions to be included, electromagnetic correction to hadronic operators at all orders and all factorizable and nonfactorizable contributions to the decay.

We write the most general form factors and amplitudes in Sec. II based only on Lorentz invariance and gauge invariance. Our approach differs from what is usually done in literature as we make no attempt to evaluate hadronic parameters but eliminate them in favor of measured observables to the extent possible. Hence, our conclusions are not limited in general by the order of accuracy up to which the calculations are done.

The decay is described by six transversity amplitudes which survive in the massless lepton case. If the mass of the lepton is finite yet another amplitude contributes to the decay. We have shown in Sec. V that the corrections to the amplitude arising from finite lepton mass can be determined completely from observables measured using angular analysis. These contributions are suppressed by m^2/q^2 and may be difficult to measure. A theoretical estimate also shows that they are insignificant in all but the first bin. We therefore began by focusing attention on the massless case which is described by the six transversity amplitudes alone. The massive lepton case was considered later to derive an exact relation valid in the SM limit. Even if the mass effects are too tiny to distinguish an attempt to measure them would ensure that the predictions are reliable and free from theoretical parameters.

We started by writing the most general parametric form of the transversity amplitude in the SM given in Eq. (17) that takes into account comprehensively all the contributions within SM. Unlike the derivations in Ref. [2] the general transversity amplitude is now allowed to be complex, by introducing three additional parameters ε_λ. This, however, poses no problem since there are three extra observables A_7, A_8 and A_9 given in Sec. III, which are nonvanishing in the complex transversity amplitudes limit. Hence, dealing with complex amplitude introduces only a technical difficulty of solving for additional variables iteratively.

Using this general amplitude a new relation [see Eq. (80)] involving all the nine CP conserving observables is derived in Sec. IV, that is exact in the SM limit assuming massless leptons. The new derivation incorporates the effect of electromagnetic correction of hadronic operators to all orders and all factorizable and nonfactorizable contributions including resonance effects to the decay. In addition to the nine observables, this new relation depends only on one form-factors ratio: P_1. The new relation becomes independent of P_1 and reduces to the one derived in Ref. [2] in the limit that the asymmetries A_7, A_8 and A_9 are all zero.

As mentioned repeatedly the inclusion of lepton mass contribution is trivial in our approach; the effect on all the observables is directly obtained in terms of asymmetries given in Eqs. (89) and (90) that can be measured as shown in Sec. V. The new relation obtained is generalized to include the lepton mass effects in Eq. (111). It is important to note that it involves only observables and the form-factor ratio P_1 and is free from any assumption within the SM framework. This relation also implies three inequalities given in Eqs. (113a)–(113c) which impose constraints on the parameter space of observables. We also presented three new relations between the observables that are exact at the zero crossings of angular asymmetries $A_{\rm FB}^{\rm o}$, $A_5^{\rm o}$ and $A_{\rm FB}^{\rm o} + \sqrt{2} A_5^{\rm o}$. These are particularly interesting if the mass effect and the imaginary contributions to the Wilson coefficients $\hat{C}_7$ and $\hat{C}_9$ are ignored, as they reduce to

simple form presented in Eq. (115). Another interesting aspect is that the form-factor ratios P_1, P_2 and P_3 can each be written in terms of observables and P_1. In the limit of vanishing A_7, A_8 and A_9 (i.e. negligible imaginary contributions), the form-factor ratios can be measured purely in terms of helicity fractions.

The limiting values of the observables at the minimum and maximum values of q^2 are discussed in Sec. VI based on very general arguments. It is interesting to note that at $q^2 = 4m^2$ all angular asymmetries vanish and each of the helicity fraction approaches $1/3$. At the maximum value of $q^2_{\rm max}$ similar results can be obtained.

In Sec. VII, we have highlighted the possible ways to check the consistency of the measured observables using the SM relation derived. It was noted that the inclusion of nonzero ε_λ indicating complex contributions to the amplitudes invariably reduces the allowed parameter space of the observables. Hence, in order to check the consistency of measured observables we take a conservative approach and set all the ε_λ's to be equal to zero for the analysis. This was necessary since A_7, A_8 and A_9 are all consistent with zero. The relation among the observables, hence, reduces to Eq. (80) which is in terms of six observables F_L, $F_\parallel$, $F_\perp$, $A_{\rm FB}$, A_4, A_5 and is completely free from any form-factor dependence. The χ^2 function in Eq. (125) was minimized in the 4-dimensional parameter space of the observables F_L, $F_\perp$, $A_{\rm FB}$ and A_5 to check the consistency between the experimentally measured values by varying each of them simultaneously within the permissible domain and $A_4^{\rm pred}$ was evaluated using the relation in Eq. (80). The projections of the minimized χ^2 function are studied for the various pairs of observables as shown in the contour plots of Figs. 1–3. In most of the contour plots the best fit (green) points lie at the edge of the boundaries except for the third bin. The experimental measured central values (black squares) generally lie within the contours except for the fourth and sixth bin. It is interesting to note that the best fits are always in the 1σ region perhaps validating the LHC*b* data set.

We compared the two distributions generated by experimental measurement and theoretical prediction of the observable A_4, assuming that A_7, A_8 and A_9 are all zero in Fig. 4. The number of events for the "Theory" histogram are chosen to be consistent statistically with the number of events observed by LHC*b* in the 1 fb^{-1} [5] data set for each of the bins. The mean values together with 1σ error bands are shown in Fig. 5 with a comparison between the massless and massive lepton case. It is found that lepton mass can be ignored except for the first q^2 bin. The fifth bin shows a large discrepancy whereas the other bins are in reasonable agreement. Since the A_4 distributions in Fig. 4 carry much more information than the mean and averages, we compare the two simulated distributions shown in the histograms using the Mathematica routine "DistributionFitTest" [30]. The P-values obtained by comparing the two are found to be less than 10^{-9} for each of the bins, except the second and fourth bins, where the P-values obtained are 2.54×10^{-5} and 6.47×10^{-6} respectively.

In order to understand better the role of the imaginary contributions that were earlier ignored, we have also preformed a simulation of all observables including A_7 A_8 and A_9. The solutions for $\varepsilon_\perp$, $\varepsilon_\parallel$ and ε_0 shown in Fig. 6 indicate that all the ε_λ's are consistent with zero and even the tails of $\varepsilon_\lambda^2/\Gamma_f$ do not cross 0.2. A comparison of the measured and predicted A_4 values for the six q^2 bins considering all the measured observables (including A_7, A_8 and A_9) are shown in Fig. 7. Interestingly, $A_4^{\rm pred}$ now fits better to a Gaussian distribution than the $\varepsilon_\lambda = 0$ case as indicated by a Kolmogorov-Smirnov test, implying possible imaginary contributions to the transversity amplitudes. The P-values still continue to be smaller than 10^{-9} for all the bins, except the second bin where the P-value is 6.78×10^{-3}, indicating that we reject the hypothesis that all observables are consistent with the exact SM relation of Eq. (111). Since the discrepancy seems to be the largest for the fifth bin ($14.0 \le q^2 \le 16.0$ GeV^2), we have performed a detailed comparison of the PDF curves for both the theoretically predicted values using $\varepsilon_\lambda = 0$ and $\varepsilon_\lambda \neq 0$ with the measured value of A_4 as shown in Fig. 8.

In this paper we have derived a relation among the observables by taking into account all possible effects within standard model by restricting ourselves to rely only on one hadronic input. The violation of this relation will provide a smoking gun signal of new physics. We have explicitly shown how the relation can be used to test SM, and confirm our understanding of the hadronic effects. We used the 1 fb^{-1} LHC*b* measured values of the observables to highlight the possible ways for the search of new physics that might contribute to this decay with the derived relations.

ACKNOWLEDGMENTS

The work of D. D. is supported by the DFG Research Unit FOR 1873 Quark Flavour Physics and Effective Field Theories. We thank Sheldon Stone for discussion on LHC*b* observation of $B^+ \to K^+\mu^+\mu^-$, which motivated our more detailed study.

APPENDIX A: DERIVATION OF $\mathbf{r}_\lambda$ SOLUTIONS

Here we present the derivation of $r_\parallel$, $r_\perp$ and r_0 solutions defined in Eq. (35). Starting with the first set of equations (Set-I) involving $r_\parallel$ and $r_\perp$ in terms of the observables given in Eqs. (54), (55) and (56) we have

$$r_\parallel^2 + \hat{C}_{10}^2 = \frac{F'_\parallel \Gamma_f \mathsf{P}_1^2}{2\mathcal{F}_\perp^2}, \tag{A1}$$

$$r_\perp^2 + \hat{C}_{10}^2 = \frac{F'_\perp \Gamma_f}{2\mathcal{F}_\perp^2}, \tag{A2}$$

$$\hat{C}_{10}(r_\parallel + r_\perp) = \frac{A_{\rm FB}\Gamma_f \mathsf{P}_1}{3\mathcal{F}_\perp^2}. \tag{A3}$$

Multiplying Eq. (A1) and (A2) we can write

$$\begin{aligned}\frac{F'_\parallel F'_\perp \Gamma_f^2 \mathsf{P}_1^2}{4\mathcal{F}_\perp^4} &= (r_\parallel r_\perp - \hat{C}_{10}^2)^2 + \hat{C}_{10}^2 (r_\parallel + r_\perp)^2 \\ &= (r_\parallel r_\perp - \hat{C}_{10}^2)^2 + \frac{A_{\rm FB}^2 \Gamma_f^2 \mathsf{P}_1^2}{9\mathcal{F}_\perp^4}\end{aligned}$$

hence,

$$r_\parallel r_\perp - \hat{C}_{10}^2 = \pm \frac{\Gamma_f \mathsf{P}_1}{2\mathcal{F}_\perp^2} \sqrt{F'_\parallel F'_\perp - \frac{4A_{\rm FB}^2}{9}}. \tag{A4}$$

Now expressing $\hat{C}_{10}^2$ in terms of $r_\parallel^2$ using Eq. (A1) and in terms of $r_\perp^2$ using Eq. (A2) we can write

$$\begin{aligned}2r_\parallel r_\perp - 2\hat{C}_{10}^2 &= 2r_\parallel r_\perp - \left(\frac{F'_\parallel \Gamma_f \mathsf{P}_1^2}{2\mathcal{F}_\perp^2} - r_\parallel^2\right) - \left(\frac{F'_\perp \Gamma_f}{2\mathcal{F}_\perp^2} - r_\perp^2\right) \\ &= \left[(r_\parallel + r_\perp)^2 - \frac{F'_\parallel \Gamma_f \mathsf{P}_1^2}{2\mathcal{F}_\perp^2} - \frac{F'_\perp \Gamma_f}{2\mathcal{F}_\perp^2}\right]. \end{aligned} \tag{A5}$$

Equating Eqs. (A4) and (A5) we get

$$\begin{aligned}r_\parallel + r_\perp &= \pm\left[\frac{F'_\parallel \Gamma_f \mathsf{P}_1^2}{2\mathcal{F}_\perp^2} + \frac{F'_\perp \Gamma_f}{2\mathcal{F}_\perp^2} \pm \frac{\Gamma_f \mathsf{P}_1}{2\mathcal{F}_\perp^2} Z'_1\right]^{\frac{1}{2}} \\ &= \frac{\pm\sqrt{\Gamma_f}}{\sqrt{2}\mathcal{F}_\perp} [\mathsf{P}_1^2 F'_\parallel + F'_\perp \pm \mathsf{P}_1 Z'_1]^{\frac{1}{2}}\end{aligned} \tag{A6}$$

where $Z'_1 = \sqrt{4F'_\parallel F'_\perp - \frac{16}{9}A_{\rm FB}^2}$. Now, Eqs. (A1) and (A2) imply

$$r_\parallel^2 - r_\perp^2 = \frac{F'_\parallel \Gamma_f \mathsf{P}_1^2}{2\mathcal{F}_\perp^2} - \frac{F'_\perp \Gamma_f}{2\mathcal{F}_\perp^2}, \tag{A7}$$

which gives $r_\parallel - r_\perp$ to be

$$r_\parallel - r_\perp = \frac{\pm\sqrt{\Gamma_f}}{\sqrt{2}\mathcal{F}_\perp} \frac{\mathsf{P}_1^2 F'_\parallel - F'_\perp}{[\mathsf{P}_1^2 F'_\parallel + F'_\perp \pm \mathsf{P}_1 Z'_1]^{\frac{1}{2}}}. \tag{A8}$$

To fix the sign ambiguity of the radical let us consider the zero crossing point of the observable $A_{\rm FB}$ where,

$$r_\parallel + r_\perp|_{A_{\rm FB}=0} = \pm\frac{\sqrt{\Gamma_f}}{\sqrt{2}\mathcal{F}_\perp}\left(\sqrt{F'_\perp} \pm \mathsf{P}_1\sqrt{F'_\parallel}\right) = 0. \tag{A9}$$

It can be easily seen from Appendix B that P_1 is always negative and thus the positive sign ambiguity has to be chosen within the radical. Solving Eqs. (A6) and (A8) we get the expressions for $r_\parallel$ and $r_\perp$ given in Eqs. (64) and (65). Similarly, following all the steps stated above for the other two sets of equations (Set-II and Set-III) we get the solutions for r_0 [in Eq. (67)] and two more expressions for the variable $r_\perp$ [Eqs. (68) and (72)].

Generalization of Eqs. (A6) and (A8) for the massive case in Sec. V is trivial from here. Below we present the explicit expressions for both massless and massive cases.

$$r_\parallel + r_\perp = \begin{cases} \frac{\pm\sqrt{\Gamma_f}}{\sqrt{2}\mathcal{F}_\perp}\left[\mathsf{P}_1^2\left(F_\parallel - \frac{2\epsilon_\parallel^2}{\Gamma_f}\right) + \left(F_\perp - \frac{2\epsilon_\perp^2}{\Gamma_f}\right) + \mathsf{P}_1 Z'_1\right]^{\frac{1}{2}} & \text{massless case} \\ \frac{\pm\sqrt{\Gamma_f^{\rm o}}}{\sqrt{2}\mathcal{F}_\perp \beta}\left[\mathsf{P}_1^2\left(F_\parallel^{\rm o} - \frac{\mathcal{T}_\parallel}{\Gamma_f^{\rm o}}\right) + \left(F_\perp^{\rm o} - \frac{\mathcal{T}_\perp}{\Gamma_f^{\rm o}}\right) + \mathsf{P}_1 Z_1^{\rm o}\right]^{\frac{1}{2}} & \text{massive case} \end{cases} \tag{A10}$$

$$r_\parallel - r_\perp = \begin{cases} \frac{\pm\sqrt{\Gamma_f}}{\sqrt{2}\mathcal{F}_\perp} \frac{\mathsf{P}_1^2\left(F_\parallel - \frac{2\epsilon_\parallel^2}{\Gamma_f}\right) - \left(F_\perp - \frac{2\epsilon_\perp^2}{\Gamma_f}\right)}{\left[\mathsf{P}_1^2\left(F_\parallel - \frac{2\epsilon_\parallel^2}{\Gamma_f}\right) + \left(F_\perp - \frac{2\epsilon_\perp^2}{\Gamma_f}\right) + \mathsf{P}_1 Z'_1\right]^{\frac{1}{2}}} & \text{massless case} \\ \frac{\pm\sqrt{\Gamma_f^{\rm o}}}{\sqrt{2}\mathcal{F}_\perp \beta} \frac{\mathsf{P}_1^2\left(F_\parallel^{\rm o} - \frac{\mathcal{T}_\parallel}{\Gamma_f^{\rm o}}\right) - \left(F_\perp^{\rm o} - \frac{\mathcal{T}_\perp}{\Gamma_f^{\rm o}}\right)}{\left[\mathsf{P}_1^2\left(F_\parallel^{\rm o} - \frac{\mathcal{T}_\parallel}{\Gamma_f^{\rm o}}\right) + \left(F_\perp^{\rm o} - \frac{\mathcal{T}_\perp}{\Gamma_f^{\rm o}}\right) + \mathsf{P}_1 Z_1^{\rm o}\right]^{\frac{1}{2}}} & \text{massive case} \end{cases} \tag{A11}$$

Using Eqs. (A3) and (A10) we can write

$$\hat{C}_{10} = \begin{cases} \frac{\pm A_{\rm FB}\sqrt{2\Gamma_f}\mathsf{P}_1}{3\mathcal{F}_\perp\left[\mathsf{P}_1^2\left(F_\parallel - \frac{2\epsilon_\parallel^2}{\Gamma_f}\right) + \left(F_\perp - \frac{2\epsilon_\perp^2}{\Gamma_f}\right) + \mathsf{P}_1 Z_1'\right]^{\frac{1}{2}}} & \text{massless case} \\ \frac{\pm A_{\rm FB}^{\rm o}\sqrt{2\Gamma_f^{\rm o}}\mathsf{P}_1}{3\mathcal{F}_\perp\left[\mathsf{P}_1^2\left(F_\parallel^{\rm o} - \frac{\mathcal{T}_\parallel}{\Gamma_f^{\rm o}}\right) + \left(F_\perp^{\rm o} - \frac{\mathcal{T}_\perp}{\Gamma_f^{\rm o}}\right) + \mathsf{P}_1 Z_1^{\rm o}\right]^{\frac{1}{2}}} & \text{massive case} \end{cases} \tag{A12}$$

APPENDIX B: FORM FACTORS

The form factors $\mathcal{F}_\lambda$ and $\tilde{\mathcal{G}}_\lambda$ can be related to the form factors $\mathcal{X}_i$ and $\mathcal{Y}_i$ introduced in Eqs. (3) and (4) by comparing the expressions for $\mathcal{A}_\lambda^{L,R}$ in Eqs. (15a)–(15c) with Eq. (17) as follows:

$$\mathcal{F}_\perp = N\sqrt{2}\sqrt{\lambda(m_B^2, m_{K^*}^2, q^2)}\mathcal{X}_3, \tag{B1a}$$

$$\tilde{\mathcal{G}}_\perp = N\sqrt{2}\sqrt{\lambda(m_B^2, m_{K^*}^2, q^2)}\frac{2(m_b + m_s)}{q^2}\hat{C}_7\mathcal{Y}_3 + \cdots, \tag{B1b}$$

$$\mathcal{F}_\parallel = 2\sqrt{2}N\mathcal{X}_1, \tag{B1c}$$

$$\tilde{\mathcal{G}}_\parallel = 2\sqrt{2}N\frac{2(m_b - m_s)}{q^2}\hat{C}_7\mathcal{Y}_1 + \cdots, \tag{B1d}$$

$$\mathcal{F}_0 = \frac{N}{2m_{K^*}\sqrt{q^2}}[4k.q\mathcal{X}_1 + \lambda(m_B^2, m_{K^*}^2, q^2)\mathcal{X}_2], \tag{B1e}$$

$$\tilde{\mathcal{G}}_0 = \frac{N}{2m_{K^*}\sqrt{q^2}}\frac{2(m_b - m_s)}{q^2} \times \hat{C}_7[4k.q\mathcal{Y}_1 + \lambda(m_B^2, m_{K^*}^2, q^2)\mathcal{Y}_2] + \cdots, \tag{B1f}$$

where these $\mathcal{X}_i$'s and $\mathcal{Y}_i$'s can be related to the well-known form factors V, $A_{0,1,2}$ and $T_{1,2,3}$ by comparing with Ref. [6] which are known up to next-to-next-to-leading order in HQET. However, it should be noted that the $\mathcal{F}_\lambda$ and $\tilde{\mathcal{G}}_\lambda$ values are not directly used anywhere throughout our paper. Only the value of P_1 is used to solve for ε_λ using Eqs. (108)–(110).

$$\mathcal{X}_0 = -\frac{2m_{K^*}}{q^2}A_0(q^2), \tag{B2a}$$

$$\mathcal{X}_1 = -\frac{1}{2}(m_B + m_{K^*})A_1(q^2), \tag{B2b}$$

$$\mathcal{X}_2 = \frac{A_2(q^2)}{m_B + m_{K^*}}, \tag{B2c}$$

$$\mathcal{X}_3 = \frac{V(q^2)}{m_B + m_{K^*}}, \tag{B2d}$$

$$\mathcal{Y}_1 = \frac{1}{2}(m_B^2 - m_{K^*}^2)T_2(q^2), \tag{B2e}$$

$$\mathcal{Y}_2 = -T_2(q^2) - \frac{q^2}{m_B^2 - m_{K^*}^2}T_3(q^2), \tag{B2f}$$

$$\mathcal{Y}_3 = -T_1(q^2). \tag{B2g}$$

Here a point to be noted that as the form factors A_1 and A_2 are always positive the ratio

$$\frac{2k.q(m_B + m_{K^*})^2}{\lambda(m_B^2, m_{K^*}^2, q^2)}\frac{A_1}{A_2} \geq 0 \tag{B3}$$

giving rise to the fact that $\mathcal{F}_\parallel$ and $\mathcal{F}_0$ always have the same sign which is negative.

[1] F. Kruger, L. M. Sehgal, N. Sinha, and R. Sinha, Phys. Rev. D **61**, 114028 (2000).
[2] D. Das and R. Sinha, Phys. Rev. D **86**, 056006 (2012); arXiv:1202.5105.
[3] R. Sinha, arXiv:hep-ph/9608314.
[4] N. Isgur and M. B. Wise, Phys. Lett. B **232**, 113 (1989); **237**, 527 (1990).
[5] R. Aaij *et al.* (LHCb Collaboration), Phys. Rev. Lett. **108**, 181806 (2012); J. High Energy Phys. 08 (2013) 131; Phys. Rev. Lett. **111**, 191801 (2013).
[6] M. Beneke, T. Feldmann, and D. Seidel, Nucl. Phys. **B612**, 25 (2001).
[7] C. Bobeth, M. Misiak, and J. Urban, Nucl. Phys. **B574**, 291 (2000).
[8] W. Altmannshofer, P. Ball, A. Bharucha, A. J. Buras, D. M. Straub, and M. Wick, J. High Energy Phys. 01 (2009) 019.
[9] G. Buchalla, A. J. Buras, and M. E. Lautenbacher, Rev. Mod. Phys. **68**, 1125 (1996).
[10] T. Hurth and M. Nakao, Annu. Rev. Nucl. Part. Sci. **60**, 645 (2010).
[11] A. J. Buras, arXiv:1102.5650.
[12] A. J. Buras and M. Munz, Phys. Rev. D **52**, 186 (1995).
[13] P. Ball and V. M. Braun, Phys. Rev. D **58**, 094016 (1998); P. Ball and R. ZwickyPhys. Rev. D**71**, 014029 (2005).

[14] R. Aaij *et al.* (LHCb Collaboration), Phys. Rev. Lett. **111**, 112003 (2013).
[15] J. Lyon and R. Zwicky, arXiv:1406.0566.
[16] A. Khodjamirian, Th. Mannel, A. A. Pivovarov, and Y.-M. Wang, J. High Energy Phys. 09 (2010) 089; A. Khodjamirian, arXiv:1312.6480.
[17] B. Grinstein and D. Prijol, Phys. Rev. D **70**, 114005 (2004).
[18] B. Grinstein, M. J. Savage, and M. B. Wise, Nucl. Phys. **B319**, 271 (1989).
[19] M. Beneke and T. Feldmann, Nucl. Phys. **B592**, 3 (2000).
[20] J. T. Wei *et al.* (BELLE Collaboration), Phys. Rev. Lett. **103**, 171801 (2009).
[21] B. Aubert *et al.* (*BABAR* Collaboration), Phys. Rev. D **79**, 031102 (2009).
[22] B. Aubert *et al.* (*BABAR* Collaboration), Phys. Rev. D **73**, 092001 (2006).
[23] CMS Collaboration, Phys. Lett. B **727**, 77 (2013)
[24] T. Aaltonen *et al.* (CDF Collaboration), Phys. Rev. Lett. **106**, 161801 (2011).
[25] T. Aaltonen *et al.* (CDF Collaboration), Phys. Rev. Lett. **107**, 201802 (2011).
[26] T. Aaltonen *et al.* (CDF Collaboration), Phys. Rev. Lett. **108**, 081807 (2012).
[27] J. Charles, A. Le Yaouanc, L. Oliver, O. Pene, and J. C. Raynal, Phys. Rev. D **60**, 014001 (1999).
[28] G. Hiller and R. Ziwcky, J. High Energy Phys. 03 (2014) 042.
[29] Wolfram Research, Inc., Mathematica, Version 10.0, Champaign, IL, 2014.
[30] Details of the routine can be found at http://reference.wolfram.com/language/ref/DistributionFitTest.html.